Density Model for Northern Bottlenose Whale (*Hyperoodon ampullatus*) for the U.S. East Coast: Supplementary Report

Model Version 2.1

Duke University Marine Geospatial Ecology Laboratory*

2023-05-27

Citation

When citing our methodology or results generally, please cite Roberts et al. (2016, 2023). The complete references appear at the end of this document. We are preparing a new article for a peer-reviewed journal that will eventually replace those. Until that is published, those are the best general citations.

When citing this model specifically, please use this reference:

Roberts JJ, Yack TM, Cañadas A, Fujioka E, Halpin PN, Barco SG, Boisseau O, Chavez-Rosales S, Cole TVN, Cotter MP, Cummings EW, Davis GE, DiGiovanni Jr. RA, Garrison LP, Gowan TA, Jackson KA, Kenney RD, Khan CB, Lockhart GG, Lomac-MacNair KS, McAlarney RJ, McLellan WA, Mullin KD, Nowacek DP, O'Brien O, Pabst DA, Palka DL, Quintana-Rizzo E, Redfern JV, Rickard ME, White M, Whitt AD, Zoidis AM (2022) Density Model for Northern Bottlenose Whale (*Hyperoodon ampullatus*) for the U.S. East Coast, Version 2.1, 2023-05-27, and Supplementary Report. Marine Geospatial Ecology Laboratory, Duke University, Durham, North Carolina.

Copyright and License

Model Version History

Version	Date	Description
1	2015-03-06	Initial version.
1.1	2015-05-14	Updated calculation of CVs. Switched density rasters to logarithmic breaks. No changes to the model.
1.2	2015-09-26	Updated the documentation. No changes to the model. Model files released as supplementary information to Roberts et al. (2016).

*For questions or to offer feedback please contact Jason Roberts (jason.roberts@duke.edu) and Tina Yack (tina.yack@duke.edu)

(continued)

Version	Date	Description
2	2022-06-20	This model is a major update over the prior version, with substantial additional data, improved statistical methods, and an increased spatial resolution. It was released as part of the final delivery of the U.S. Navy Marine Species Density Database (NMSDD) for the Atlantic Fleet Testing and Training (AFTT) Phase IV Environmental Impact Statement. Several new collaborators joined and contributed survey data: New York State Department of Environmental Conservation, TetraTech, HDR, and Marine Conservation Research. We incorporated additional surveys from all continuing and new collaborators through the end of 2020. (Because some environmental covariates were only available through 2019, certain models only extend through 2019.) We increased the spatial resolution to 5 km and, at NOAA's request, we extended the model further inshore from New York through Maine. We reformulated and refitted all detection functions and spatial models. We updated all enviromental covariates to newer products, when available, and added several covariates to the set of candidates. For models that incorporated dynamic covariates, we estimated model uncertainty using a new method that accounts for both model parameter error and temporal variability.
2.1	2023-05-27	Completed the supplementary report documenting the details of this model. Corrected the 5 and 95 percent rasters so that they contain the value 0 where the taxon was asssumed absent, rather than NoData. Nothing else was changed.

1 Survey Data

We built this model from data collected between 1998-2020 (Table 1, Figure 1). We excluded the southeast U.S. right whale Early Warning System (EWS) surveys because they did not target beaked whales, except those by UNCW which targeted all cetaceans. To maintain consistency with the other models developed during the 2022 modeling cycle, most of which excluded data prior to 1998 in order to utilize biological covariates derived from satellite ocean color observations, we also excluded data prior to 1998 from this model. We restricted the model to aerial survey transects with sea states of Beaufort 4 or less (for a few surveys we used Beaufort 3 or less) and shipboard transects with Beaufort 5 or less (for a few we used Beaufort 4 or less). We also excluded transects with poor weather or visibility for surveys that reported those conditions.

Table 1: Survey effort and observations considered for this model. Effort is tallied as the cumulative length of on-effort transects. Observations are the number of groups and individuals encountered while on effort. Off effort observations and those lacking an estimate of group size or distance to the group were excluded.

			Effort	Observations		
Institution	Program	Period	1000s km	Groups	Individuals	Mean Group Size
Aerial Surveys						
HDR	Navy Norfolk Canyon	2018-2019	11	0	0	
NEAq	CNM	2017-2020	2	0	0	
NEAq	MMS-WEA	2017-2020	37	0	0	
NEAq	NLPSC	2011-2015	43	0	0	
NEFSC	AMAPPS	2010-2019	89	2	13	6.5
NEFSC	NARWSS	2003-2020	448	1	2	2.0
NEFSC	Pre-AMAPPS	1999-2008	46	1	2	2.0
NYS-DEC/TT	NYBWM	2017-2020	60	0	0	
SEFSC	AMAPPS	2010-2020	114	0	0	
SEFSC	MATS	2002-2005	27	0	0	
UNCW	MidA Bottlenose	2002-2002	17	0	0	
UNCW	Navy Cape Hatteras	2011-2017	34	0	0	
UNCW	Navy Jacksonville	2009-2017	92	0	0	
UNCW	Navy Norfolk Canyon	2015-2017	14	0	0	
UNCW	Navy Onslow Bay	2007-2011	49	0	0	
UNCW	SEUS NARW EWS	2005-2008	114	0	0	
VAMSC	MD DNR WEA	2013-2015	16	0	0	
VAMSC	Navy VACAPES	2016-2017	19	0	0	
VAMSC	VA CZM WEA	2012-2015	21	0	0	
		Total	**1,255**	**4**	**17**	**4.2**
Shipboard Surveys						
MCR	SOTW Visual	2012-2019	8	2	3	1.5
NEFSC	AMAPPS	2011-2016	14	0	0	
NEFSC	Pre-AMAPPS	1998-2007	11	4	16	4.0
SEFSC	AMAPPS	2011-2016	14	0	0	
SEFSC	Pre-AMAPPS	1998-2006	27	0	0	
		Total	**74**	**6**	**19**	**3.2**
		Grand Total	**1,329**	**10**	**36**	**3.6**

Table 2: Institutions that contributed surveys used in this model.

Institution	Full Name
HDR	HDR, Inc.
MCR	Marine Conservation Research
NEAq	New England Aquarium
NEFSC	NOAA Northeast Fisheries Science Center
NYS-DEC/TT	New York State Department of Environmental Conservation and Tetra Tech, Inc.
SEFSC	NOAA Southeast Fisheries Science Center

Table 2: Institutions that contributed surveys used in this model. *(continued)*

Institution	Full Name
UNCW	University of North Carolina Wilmington
VAMSC	Virginia Aquarium & Marine Science Center

Table 3: Descriptions and references for survey programs used in this model.

Program	Description	References
AMAPPS	Atlantic Marine Assessment Program for Protected Species	Palka et al. (2017), Palka et al. (2021)
CNM	Northeast Canyons Marine National Monument Aerial Surveys	Redfern et al. (2021)
MATS	Mid-Atlantic Tursiops Surveys	
MD DNR WEA	Aerial Surveys of the Maryland Wind Energy Area	Barco et al. (2015)
MidA Bottlenose	Mid-Atlantic Onshore/Offshore Bottlenose Dolphin Surveys	Torres et al. (2005)
MMS-WEA	Marine Mammal Surveys of the MA and RI Wind Energy Areas	Quintana-Rizzo et al. (2021), O'Brien et al. (2022)
NARWSS	North Atlantic Right Whale Sighting Surveys	Cole et al. (2007)
Navy Cape Hatteras	Aerial Surveys of the Navy's Cape Hatteras Study Area	McLellan et al. (2018)
Navy Jacksonville	Aerial Surveys of the Navy's Jacksonville Study Area	Foley et al. (2019)
Navy Norfolk Canyon	Aerial Surveys of the Navy's Norfolk Canyon Study Area	Cotter (2019), McAlarney et al. (2018)
Navy Onslow Bay	Aerial Surveys of the Navy's Onslow Bay Study Area	Read et al. (2014)
Navy VACAPES	Aerial Survey Baseline Monitoring in the Continental Shelf Region of the VACAPES OPAREA	Mallette et al. (2017)
NLPSC	Northeast Large Pelagic Survey Collaborative Aerial Surveys	Leiter et al. (2017), Stone et al. (2017)
NYBWM	New York Bight Whale Monitoring Surveys	Zoidis et al. (2021)
Pre-AMAPPS	Pre-AMAPPS Marine Mammal Abundance Surveys	Mullin and Fulling (2003), Garrison et al. (2010), Palka (2006)
SEUS NARW EWS	Southeast U.S. Right Whale Early Warning System Surveys	
SOTW Visual	R/V Song of the Whale Visual Surveys	Ryan et al. (2013)
VA CZM WEA	Virginia CZM Wind Energy Area Surveys	Mallette et al. (2014), Mallette et al. (2015)

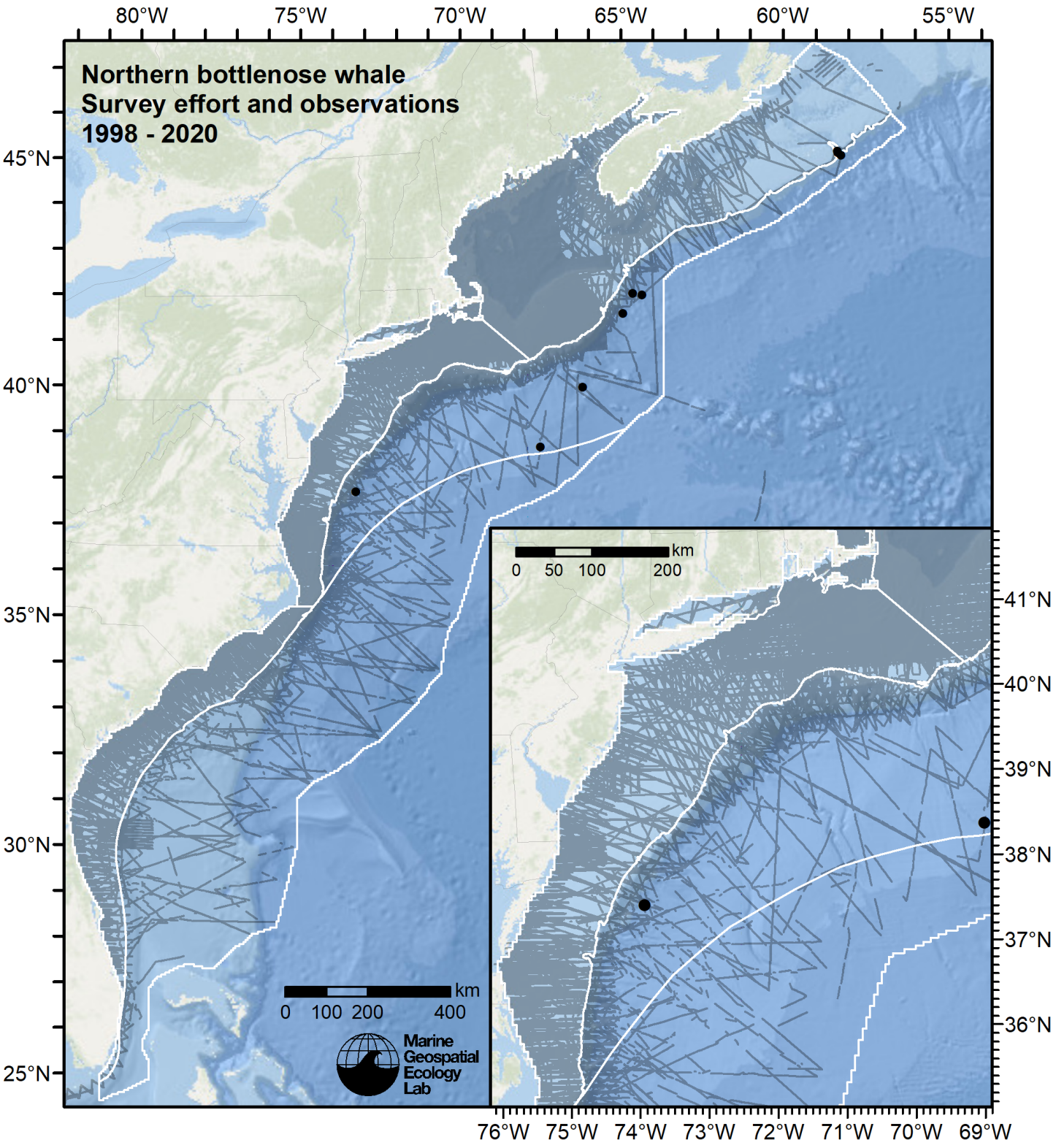

Figure 1: Survey effort and northern bottlenose whale observations available for density modeling, after detection functions were applied, and excluded segments and truncated observations were removed. White outlines show the strata for which density estimates were derived.

2 Detection Functions

2.1 With a Taxonomic Covariate

We fitted the detection functions in this section to pools of species with similar detectability characteristics and used the taxonomic identification as a covariate (ScientificName) to account for differences between them. We consulted the literature and observer teams to determine appropriate poolings. We usually employed this approach to boost the counts of observations in the detection functions, which increased the chance that other covariates such as Beaufort sea state could be used to account for differences in observing conditions. When defining the taxonomic covariate, we sometimes had too few observations of species to allocate each of them their own level of the covariate and had to group them together, again consulting the literature and observers for advice on species similarity. Also, when species were observed frequently enough to be allocated their own levels but statistical tests indicated no significant difference between the levels, we usually grouped them together into a single level.

2.1.1 Beaked and Kogia Whales

2.1.1.1 Aerial Surveys

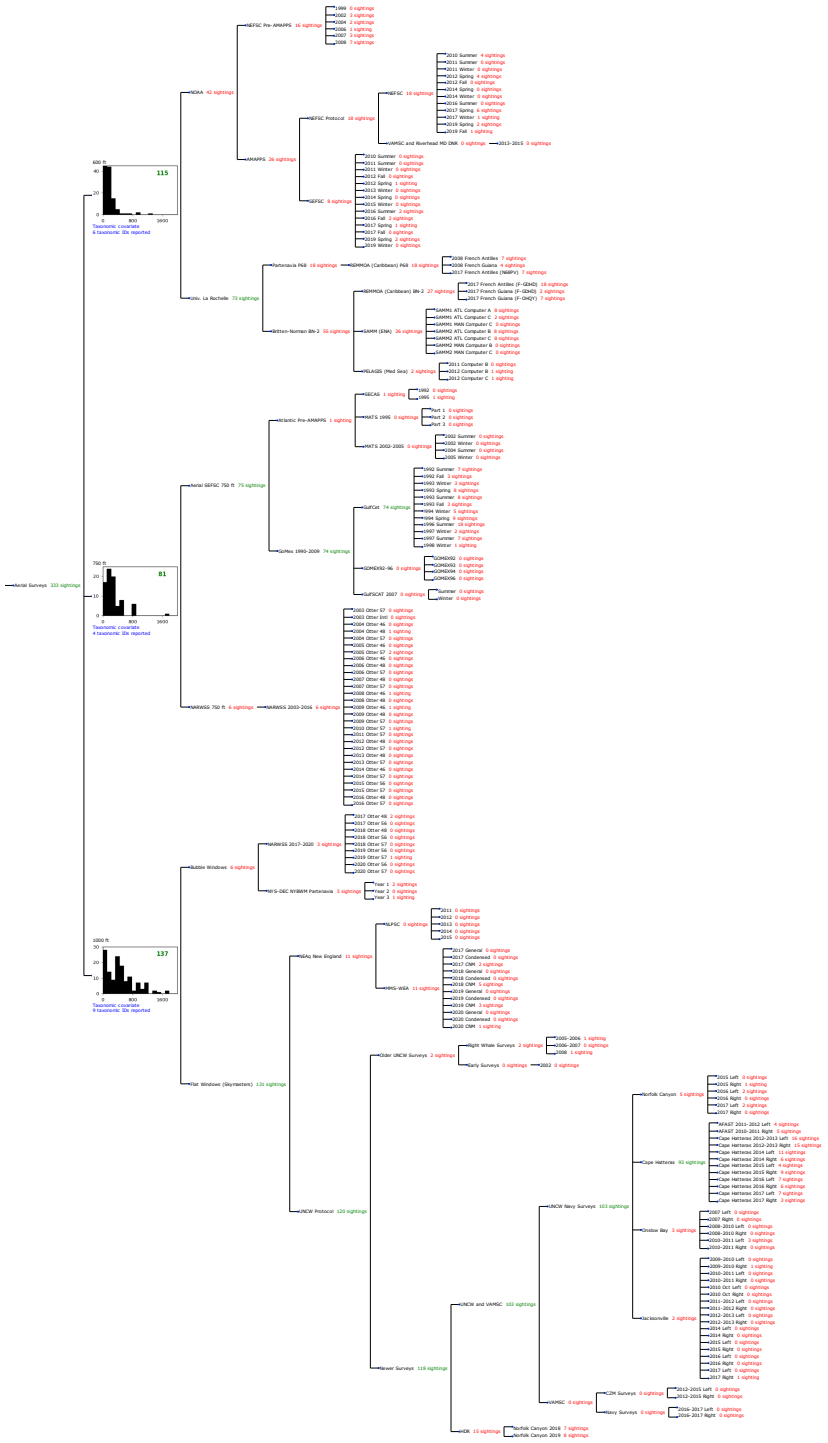

Figure 2: Detection hierarchy for aerial surveys, showing how they were pooled during detectability modeling, for detection functions that pooled multiple taxa and used used a taxonomic covariate to account for differences between them. Each histogram represents a detection function and summarizes the perpendicular distances of observations that were pooled to fit it, prior to truncation. Observation counts, also prior to truncation, are shown in green when they met the recommendation of Buckland et al. (2001) that detection functions utilize at least 60 sightings, and red otherwise. For rare taxa, it was not always possible to meet this recommendation, yielding higher statistical uncertainty. During the spatial modeling stage of the analysis, effective strip widths were computed for each survey using the closest detection function above it in the hierarchy (i.e. moving from right to left in the figure). Surveys that do not have a detection function above them in this figure were either addressed by a detection function presented in a different section of this report, or were omitted from the analysis.

2.1.1.1.1 600 ft

After right-truncating observations greater than 400 m, we fitted the detection function to the 109 observations that remained (Table 4). The selected detection function (Figure 3) used a hazard rate key function with OriginalScientificName (Figure 4) as a covariate.

Table 4: Observations used to fit the 600 ft detection function.

ScientificName	n
Hyperoodon ampullatus	3
Kogia	23
Mesoplodon	14
Mesoplodon bidens	1
Ziphiidae	33
Ziphius cavirostris	35
Total	**109**

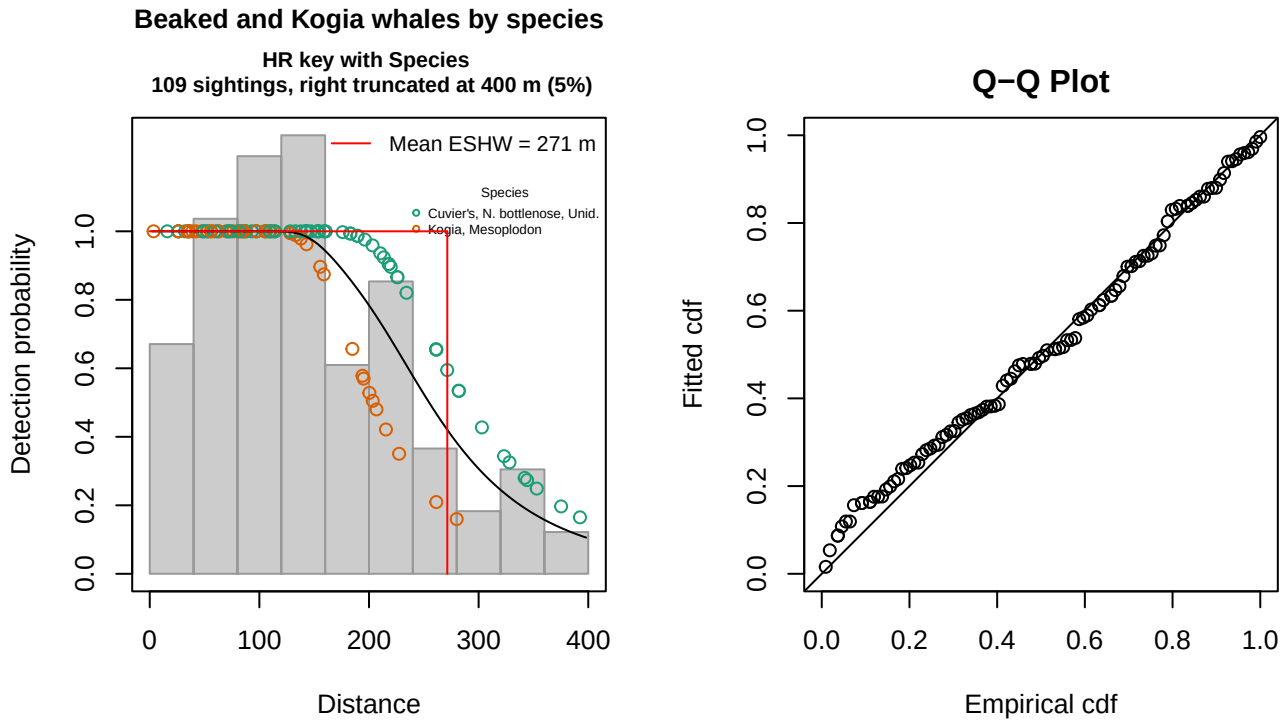

Figure 3: 600 ft detection function and Q-Q plot showing its goodness of fit.

Statistical output for this detection function:

```
Summary for ds object
Number of observations :  109
Distance range         :  0  -  400
AIC                    :  1272.901

Detection function:
 Hazard-rate key function

Detection function parameters
Scale coefficient(s):
                                    estimate        se
(Intercept)                      5.5800164 0.1212472
```

```
OriginalScientificNameKogia, Mesoplodon -0.3454612 0.1492241

Shape coefficient(s):
            estimate        se
(Intercept) 1.474338 0.3977595

                        Estimate          SE         CV
Average p             0.6645919  0.04555694 0.06854874
N in covered region 164.0104361 14.58154672 0.08890621

Distance sampling Cramer-von Mises test (unweighted)
Test statistic = 0.116256  p = 0.510907
```

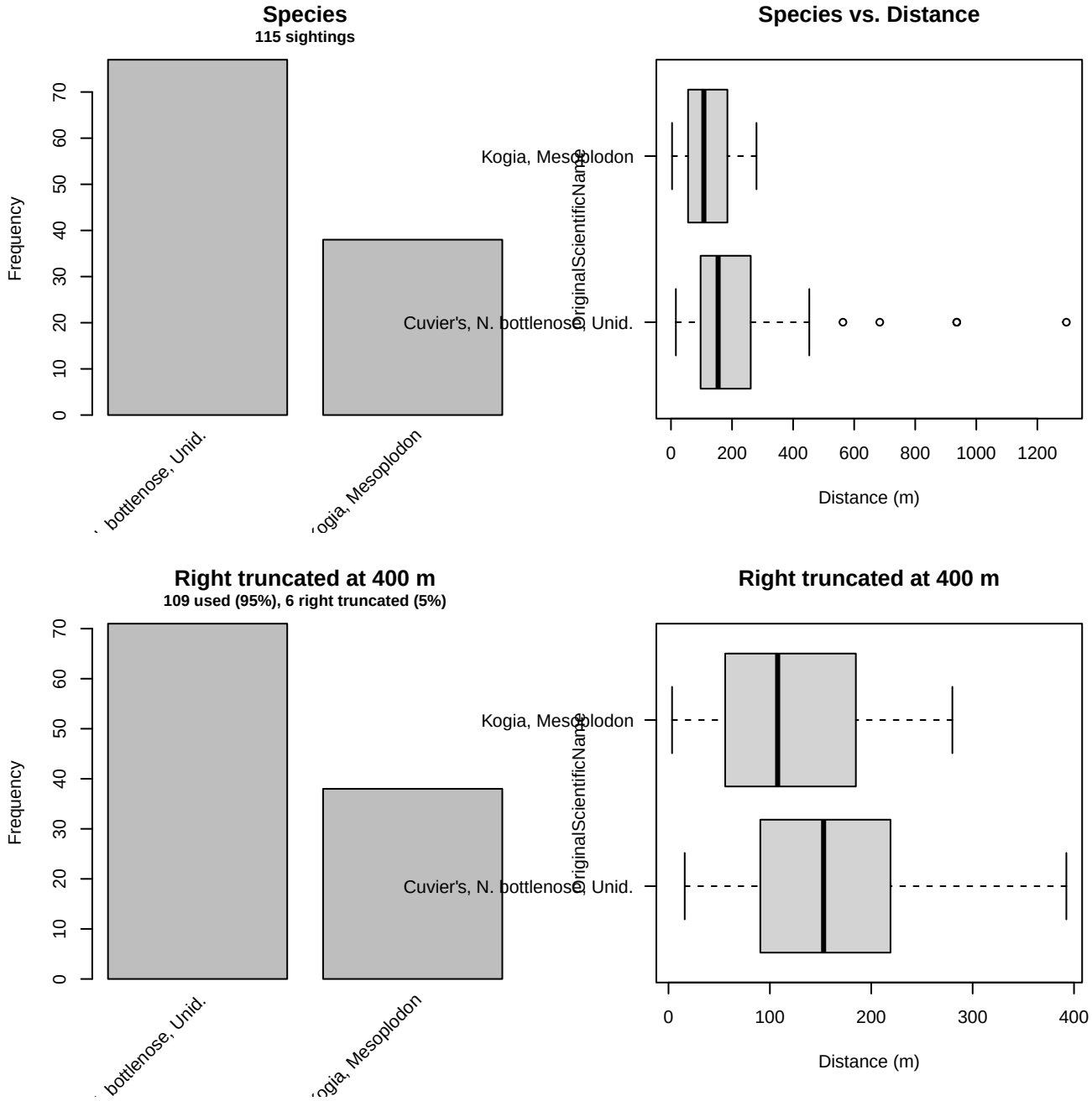

Figure 4: Distribution of the OriginalScientificName covariate before (top row) and after (bottom row) observations were truncated to fit the 600 ft detection function.

2.1.1.1.2 750 ft

After right-truncating observations greater than 1297 m, we fitted the detection function to the 80 observations that remained (Table 5). The selected detection function (Figure 5) used a hazard rate key function with Beaufort (Figure 6) and OriginalScientificName (Figure 7) as covariates.

Table 5: Observations used to fit the 750 ft detection function.

ScientificName	n
Kogia	55
Mesoplodon	9
Ziphiidae	12
Ziphius cavirostris	4
Total	**80**

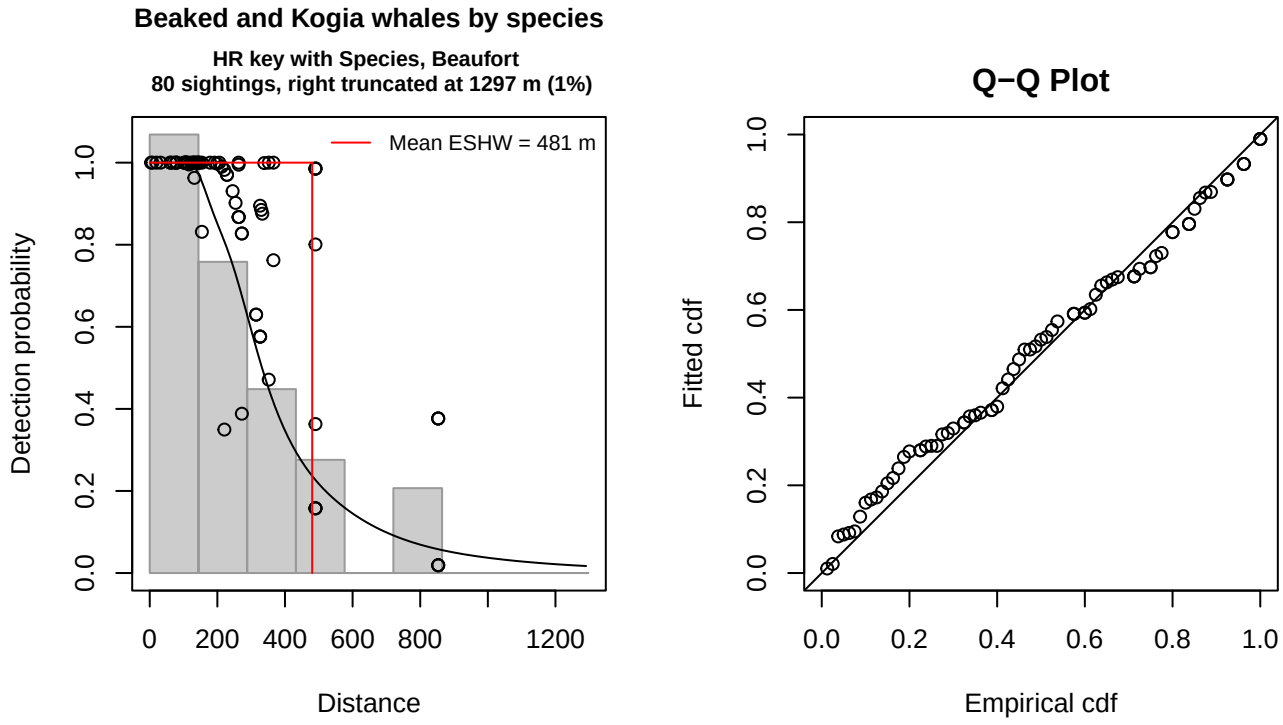

Figure 5: 750 ft detection function and Q-Q plot showing its goodness of fit.

Statistical output for this detection function:

```
Summary for ds object
Number of observations :  80
Distance range         :  0  -  1297
AIC                    :  1037.791

Detection function:
 Hazard-rate key function

Detection function parameters
Scale coefficient(s):
                             estimate        se
(Intercept)                 7.1253756 0.3142159
OriginalScientificNameKogia -0.8097794 0.2203485
Beaufort                    -0.5658239 0.1695498
```

```
Shape coefficient(s):
            estimate        se
(Intercept) 1.375855 0.1977036

                        Estimate          SE        CV
Average p              0.3064062  0.03275229 0.1068917
N in covered region 261.0913218 37.74245080 0.1445565

Distance sampling Cramer-von Mises test (unweighted)
Test statistic = 0.106921  p = 0.551997
```

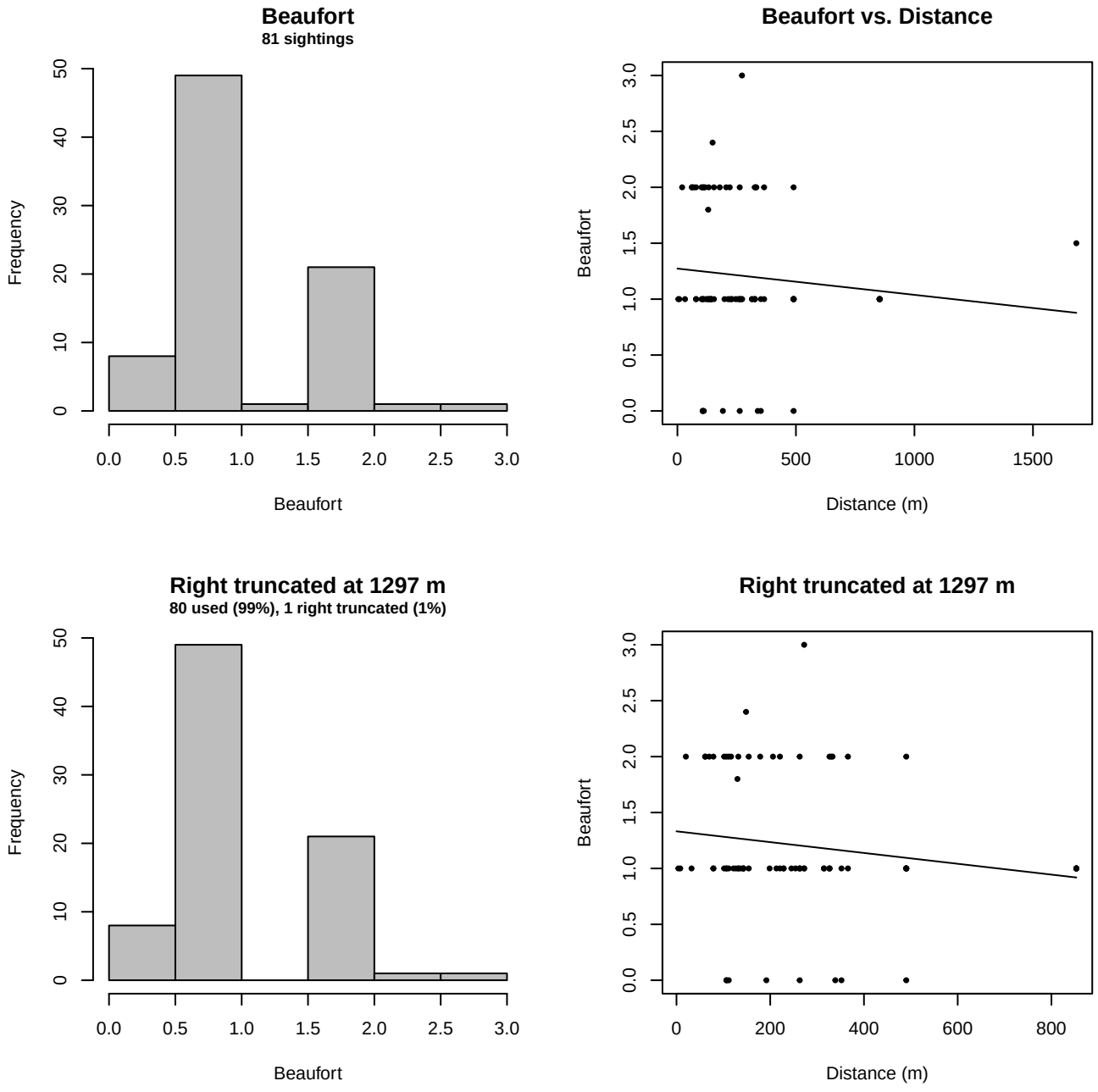

Figure 6: Distribution of the Beaufort covariate before (top row) and after (bottom row) observations were truncated to fit the 750 ft detection function.

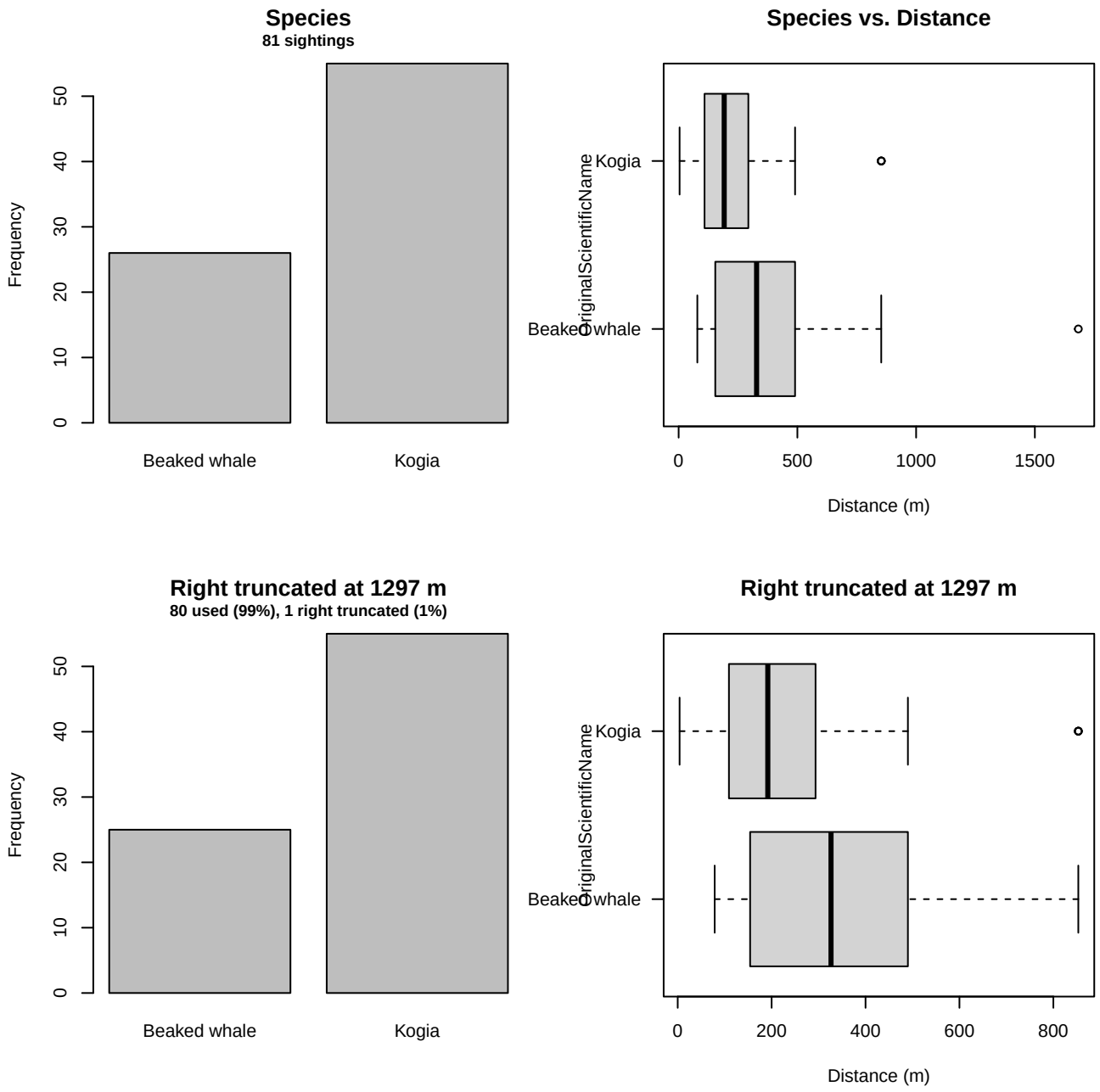

Figure 7: Distribution of the OriginalScientificName covariate before (top row) and after (bottom row) observations were truncated to fit the 750 ft detection function.

2.1.1.1.3 1000 ft

After right-truncating observations greater than 1250 m, we fitted the detection function to the 131 observations that remained (Table 6). The selected detection function (Figure 8) used a half normal key function with OriginalScientificName (Figure 9) as a covariate.

Table 6: Observations used to fit the 1000 ft detection function.

ScientificName	n
Hyperoodon ampullatus	1
Kogia	14
Kogia sima	1
Mesoplodon	26
Mesoplodon bidens	6
Mesoplodon europaeus	7
Mesoplodon mirus	3
Ziphiidae	11
Ziphius cavirostris	62
Total	**131**

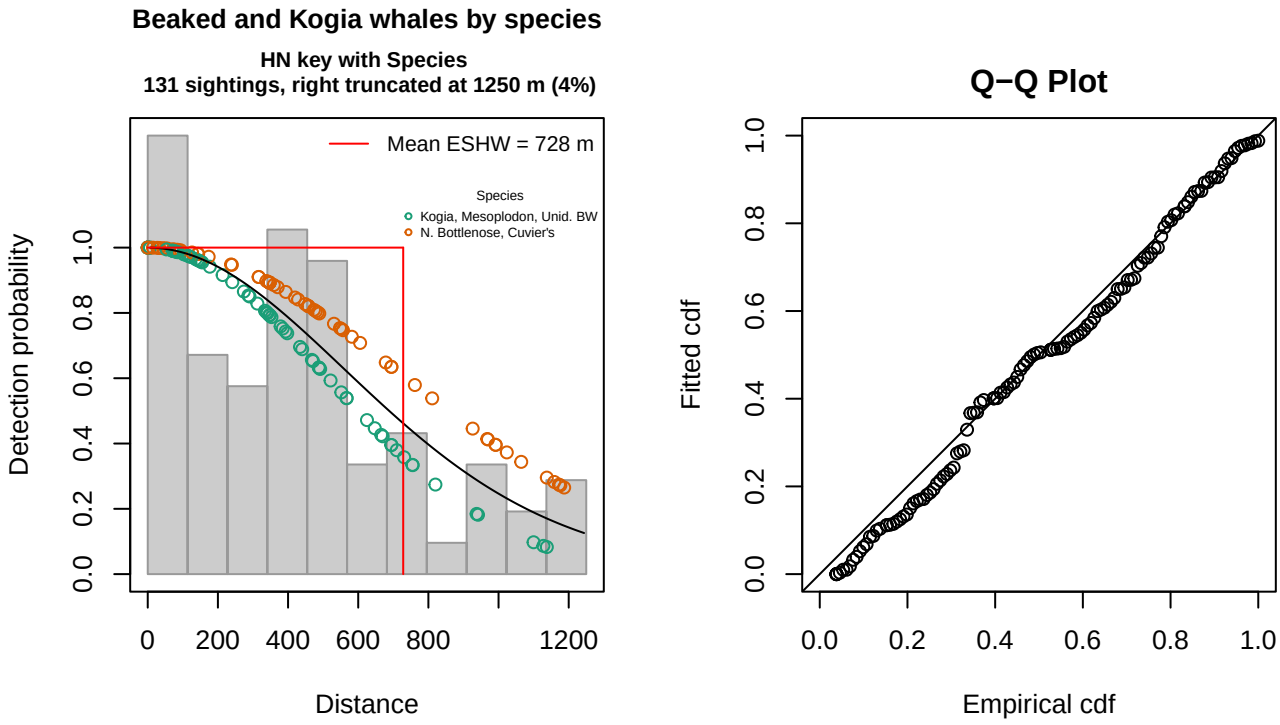

Figure 8: 1000 ft detection function and Q-Q plot showing its goodness of fit.

Statistical output for this detection function:

```
Summary for ds object
Number of observations :  131
Distance range         :  0  -  1250
AIC                    :  1830.819

Detection function:
 Half-normal key function

Detection function parameters
Scale coefficient(s):
                                          estimate        se
(Intercept)                              6.2340705 0.1031336
OriginalScientificNameN. Bottlenose, Cuvier's 0.3570255 0.1899459

                     Estimate          SE         CV
```

```
Average p             0.5712474  0.04000868 0.07003740
N in covered region 229.3227075 20.84792919 0.09091088

Distance sampling Cramer-von Mises test (unweighted)
Test statistic = 0.133457  p = 0.444164
```

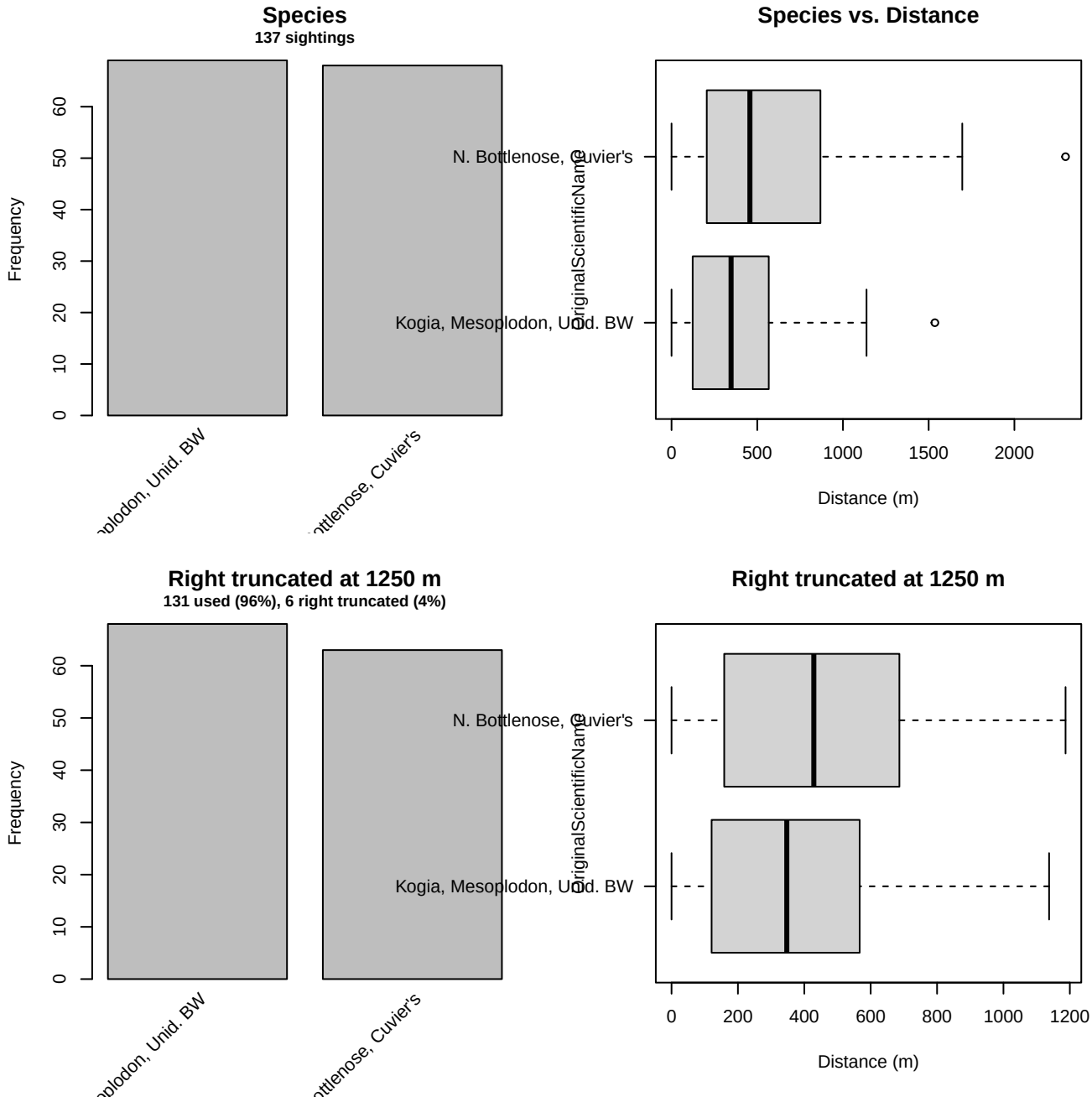

Figure 9: Distribution of the OriginalScientificName covariate before (top row) and after (bottom row) observations were truncated to fit the 1000 ft detection function.

2.1.1.2 Shipboard Surveys

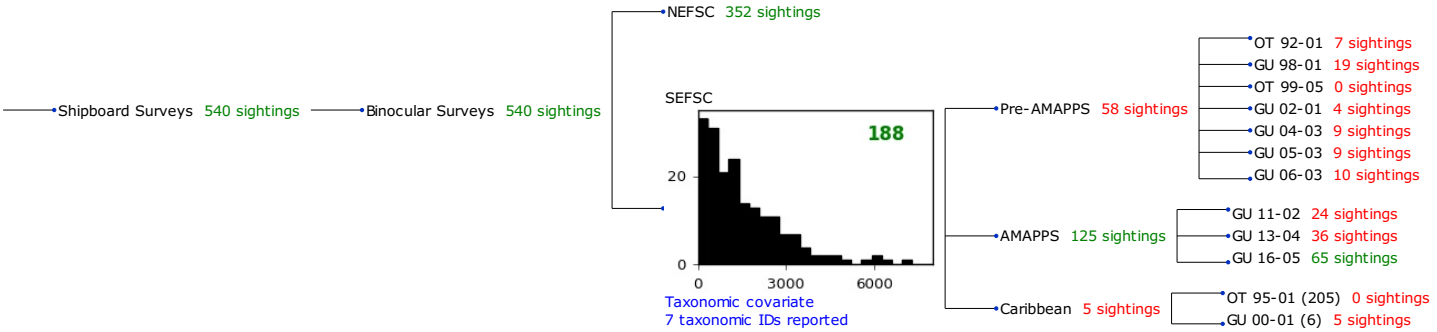

Figure 10: Detection hierarchy for shipboard surveys, showing how they were pooled during detectability modeling, for detection functions that pooled multiple taxa and used used a taxonomic covariate to account for differences between them. Each histogram represents a detection function and summarizes the perpendicular distances of observations that were pooled to fit it, prior to truncation. Observation counts, also prior to truncation, are shown in green when they met the recommendation of Buckland et al. (2001) that detection functions utilize at least 60 sightings, and red otherwise. For rare taxa, it was not always possible to meet this recommendation, yielding higher statistical uncertainty. During the spatial modeling stage of the analysis, effective strip widths were computed for each survey using the closest detection function above it in the hierarchy (i.e. moving from right to left in the figure). Surveys that do not have a detection function above them in this figure were either addressed by a detection function presented in a different section of this report, or were omitted from the analysis.

2.1.1.2.1 SEFSC

After right-truncating observations greater than 5000 m, we fitted the detection function to the 182 observations that remained (Table 7). The selected detection function (Figure 11) used a half normal key function with Beaufort (Figure 12) and OriginalScientificName (Figure 13) as covariates.

Table 7: Observations used to fit the SEFSC detection function.

ScientificName	n
Kogia	60
Kogia sima	9
Mesoplodon	37
Mesoplodon densirostris	3
Mesoplodon europaeus	1
Ziphiidae	52
Ziphius cavirostris	20
Total	**182**

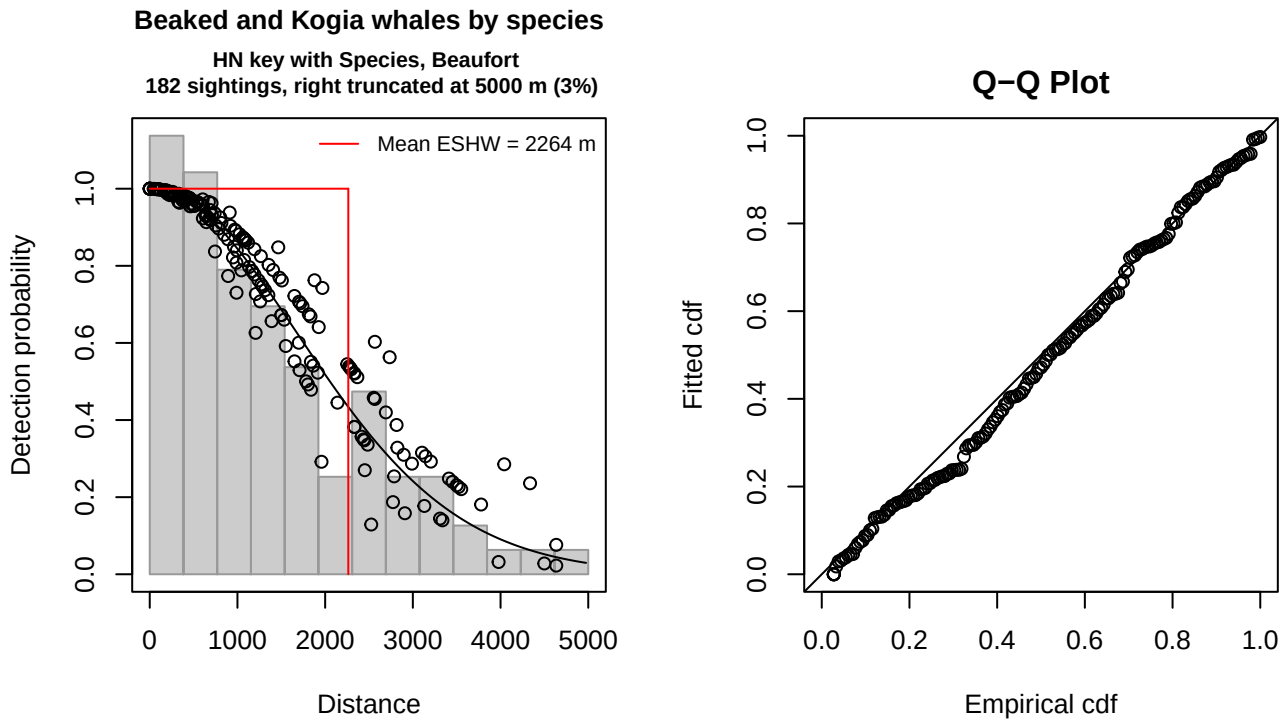

Figure 11: SEFSC detection function and Q-Q plot showing its goodness of fit.

Statistical output for this detection function:

```
Summary for ds object
Number of observations :  182
Distance range         :  0  -  5000
AIC                    :  2985.886

Detection function:
 Half-normal key function

Detection function parameters
Scale coefficient(s):
                                                              estimate
(Intercept)                                                 7.4282169
OriginalScientificNameMesoplodon spp. and Unid. beaked whale  0.1940795
OriginalScientificNameZiphius or N. bottlenose                0.4163007
Beaufort3-4                                                  -0.2991956
                                                                    se
(Intercept)                                                 0.08116764
OriginalScientificNameMesoplodon spp. and Unid. beaked whale 0.12604909
OriginalScientificNameZiphius or N. bottlenose              0.24124124
Beaufort3-4                                                 0.13661134

                      Estimate          SE         CV
Average p             0.4423162  0.02407533 0.05443013
N in covered region 411.4703239 32.09594942 0.07800307

Distance sampling Cramer-von Mises test (unweighted)
Test statistic = 0.128965  p = 0.460545
```

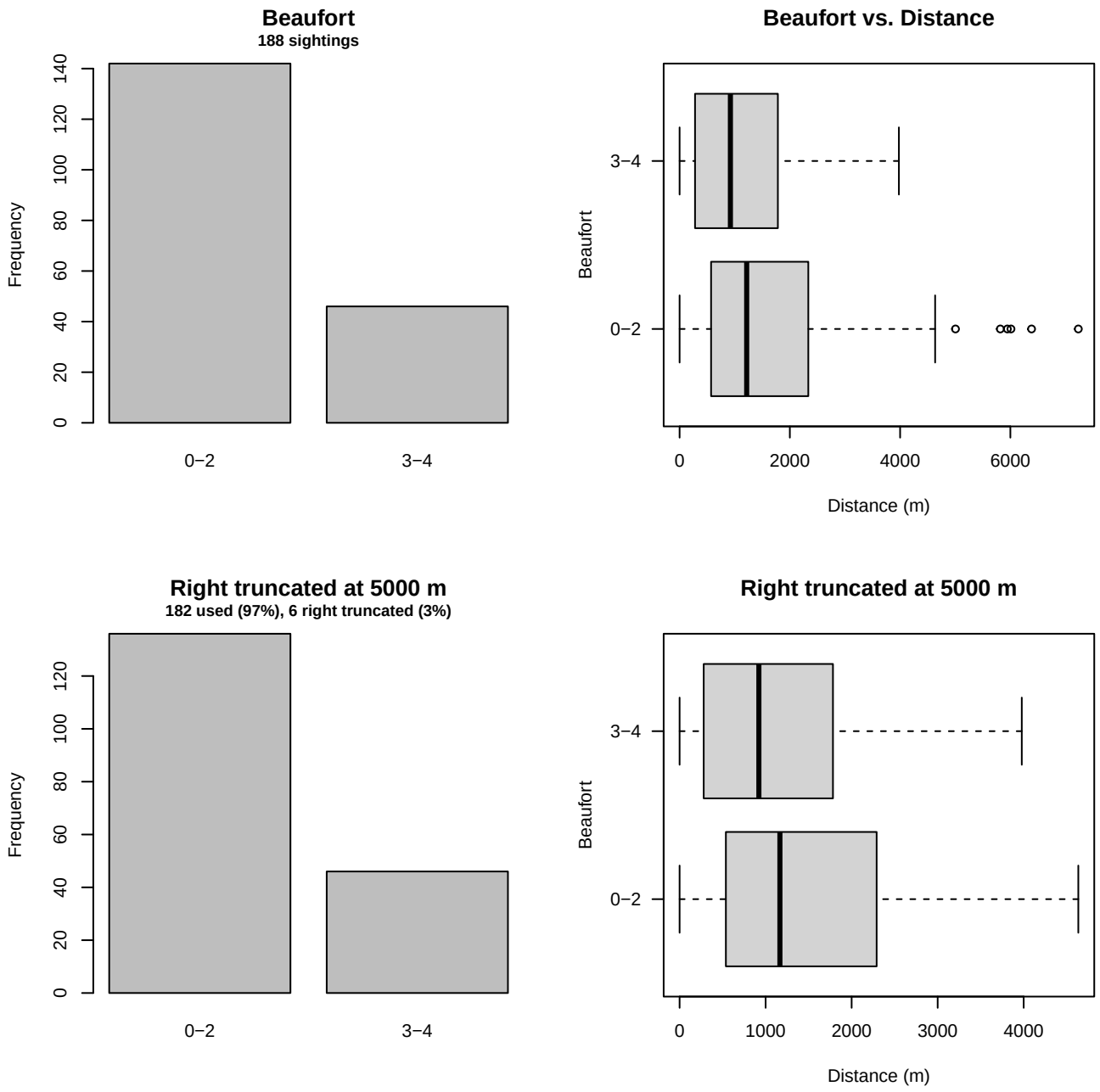

Figure 12: Distribution of the Beaufort covariate before (top row) and after (bottom row) observations were truncated to fit the SEFSC detection function.

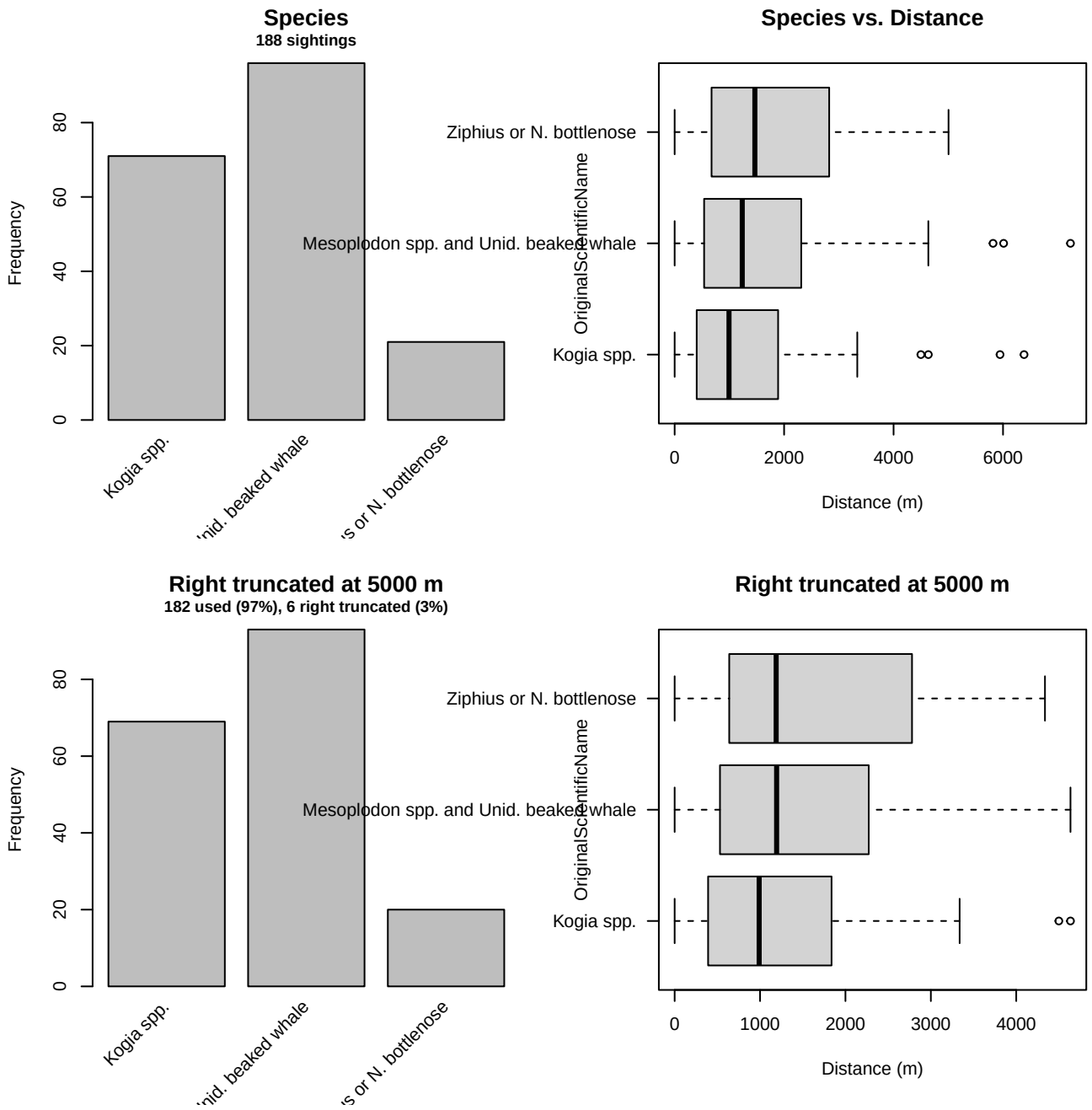

Figure 13: Distribution of the OriginalScientificName covariate before (top row) and after (bottom row) observations were truncated to fit the SEFSC detection function.

2.1.2 Beaked Whales

2.1.2.1 Shipboard Surveys

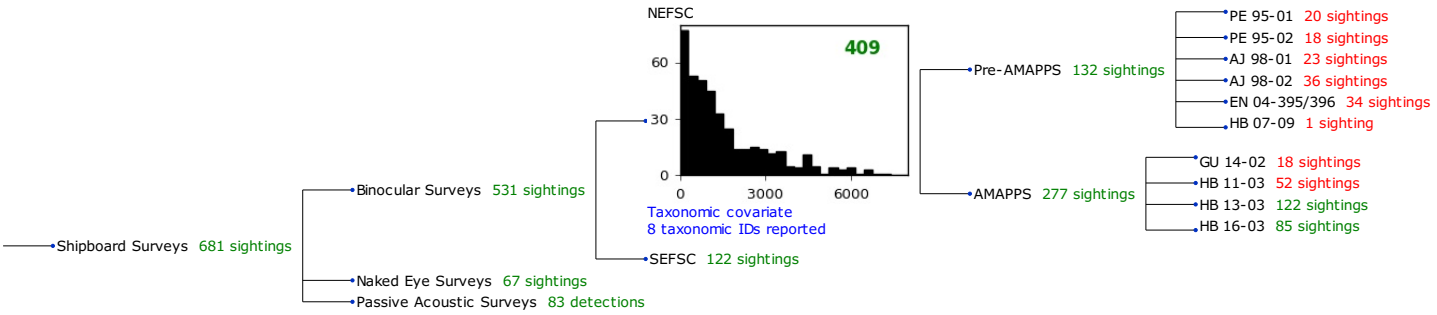

Figure 14: Detection hierarchy for shipboard surveys, showing how they were pooled during detectability modeling, for detection functions that pooled multiple taxa and used used a taxonomic covariate to account for differences between them. Each histogram represents a detection function and summarizes the perpendicular distances of observations that were pooled to fit it, prior to truncation. Observation counts, also prior to truncation, are shown in green when they met the recommendation of Buckland et al. (2001) that detection functions utilize at least 60 sightings, and red otherwise. For rare taxa, it was not always possible to meet this recommendation, yielding higher statistical uncertainty. During the spatial modeling stage of the analysis, effective strip widths were computed for each survey using the closest detection function above it in the hierarchy (i.e. moving from right to left in the figure). Surveys that do not have a detection function above them in this figure were either addressed by a detection function presented in a different section of this report, or were omitted from the analysis.

2.1.2.1.1 NEFSC

After right-truncating observations greater than 6000 m, we fitted the detection function to the 402 observations that remained (Table 8). The selected detection function (Figure 15) used a hazard rate key function with Beaufort (Figure 16), OriginalScientificName (Figure 17) and VesselName (Figure 18) as covariates.

Table 8: Observations used to fit the NEFSC detection function.

ScientificName	n
Hyperoodon ampullatus	4
Mesoplodon	69
Mesoplodon bidens	40
Mesoplodon densirostris	4
Mesoplodon europaeus	9
Mesoplodon mirus	7
Ziphiidae	147
Ziphius cavirostris	122
Total	**402**

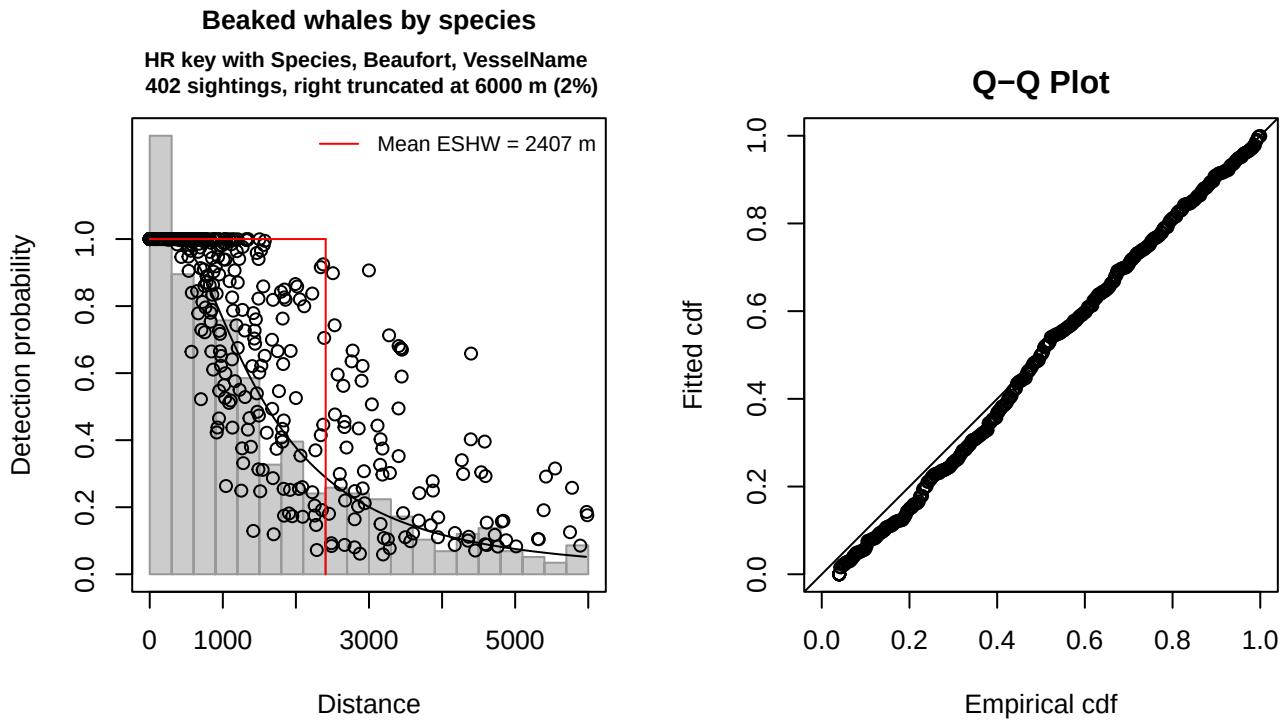

Figure 15: NEFSC detection function and Q-Q plot showing its goodness of fit.

Statistical output for this detection function:

```
Summary for ds object
Number of observations :  402
Distance range         :  0  -  6000
AIC                    :  6644.8

Detection function:
 Hazard-rate key function

Detection function parameters
Scale coefficient(s):
                                                      estimate         se
(Intercept)                                          7.2946616 0.23066680
OriginalScientificNameN. Bottlenose or Unid. beaked whale  0.4273741 0.15634310
OriginalScientificNameZiphius cavirostris            0.2066261 0.14919980
Beaufort                                            -0.3259831 0.06466977
VesselNameBigelow, Endeavor, Gunter                  0.7959452 0.15617439

Shape coefficient(s):
             estimate        se
(Intercept) 0.8157154 0.1116931

                        Estimate          SE         CV
Average p              0.3459974  0.02233711 0.06455861
N in covered region 1161.8584040 89.48657432 0.07702021

Distance sampling Cramer-von Mises test (unweighted)
Test statistic = 0.276181  p = 0.158010
```

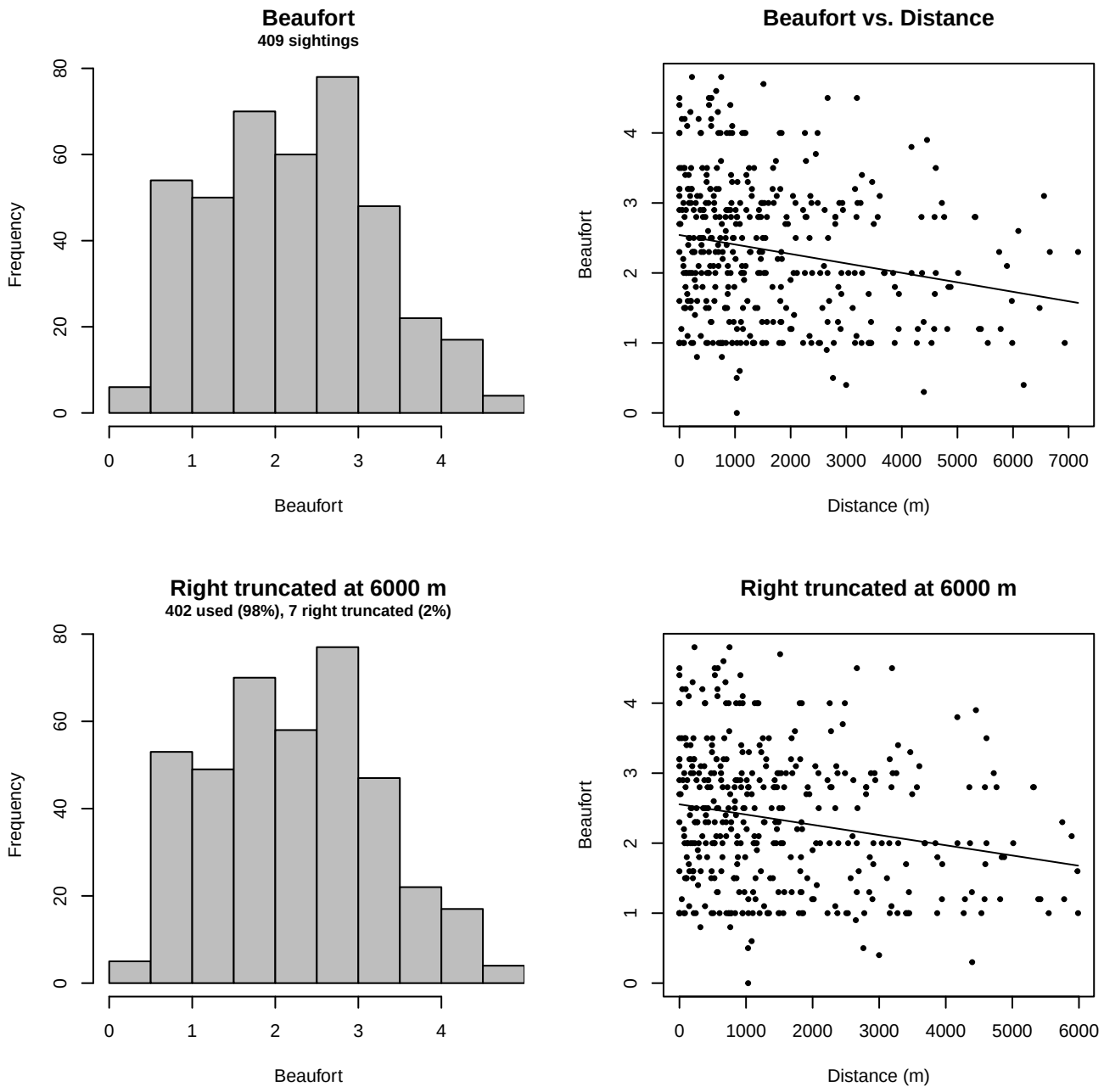

Figure 16: Distribution of the Beaufort covariate before (top row) and after (bottom row) observations were truncated to fit the NEFSC detection function.

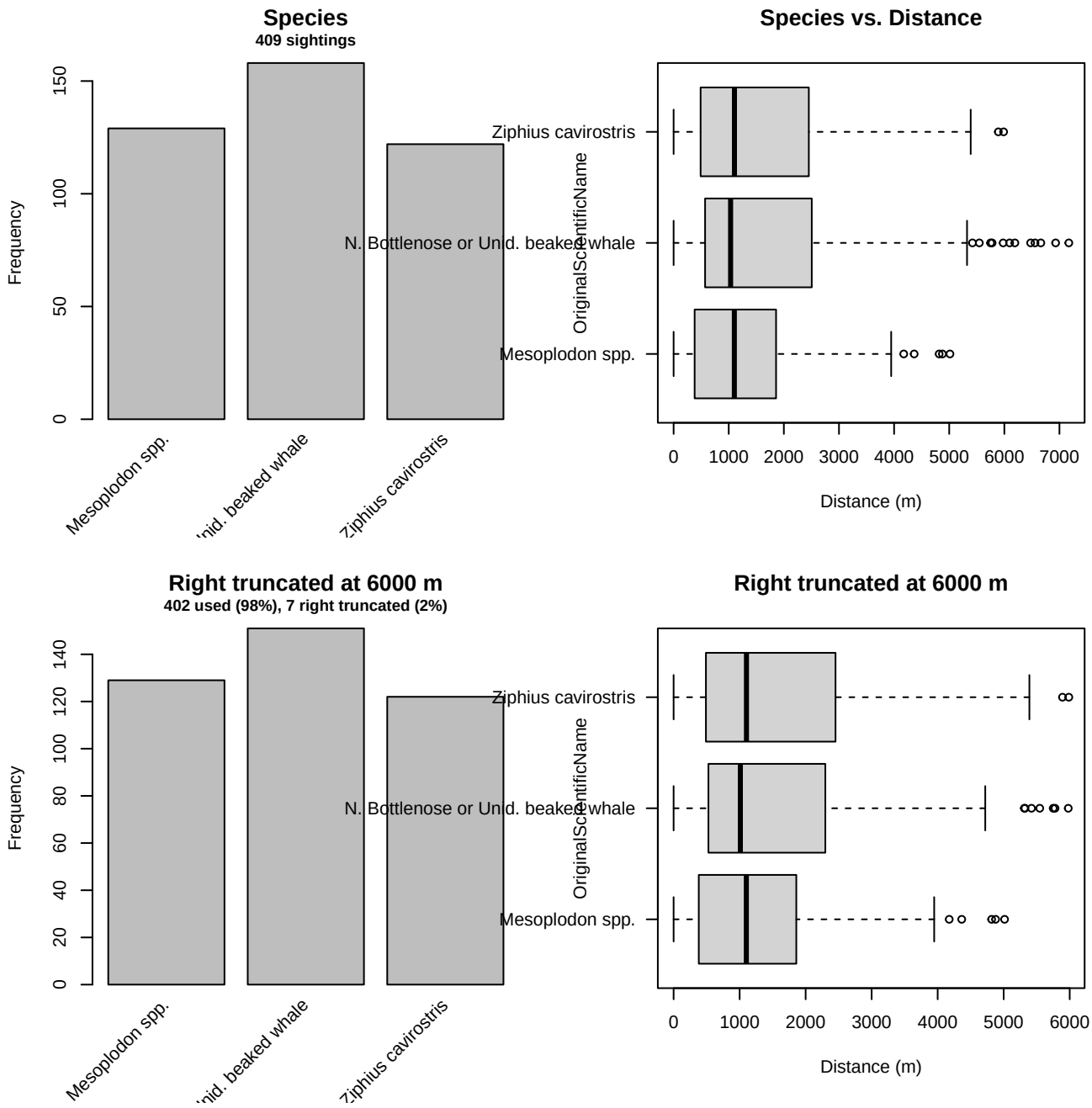

Figure 17: Distribution of the OriginalScientificName covariate before (top row) and after (bottom row) observations were truncated to fit the NEFSC detection function.

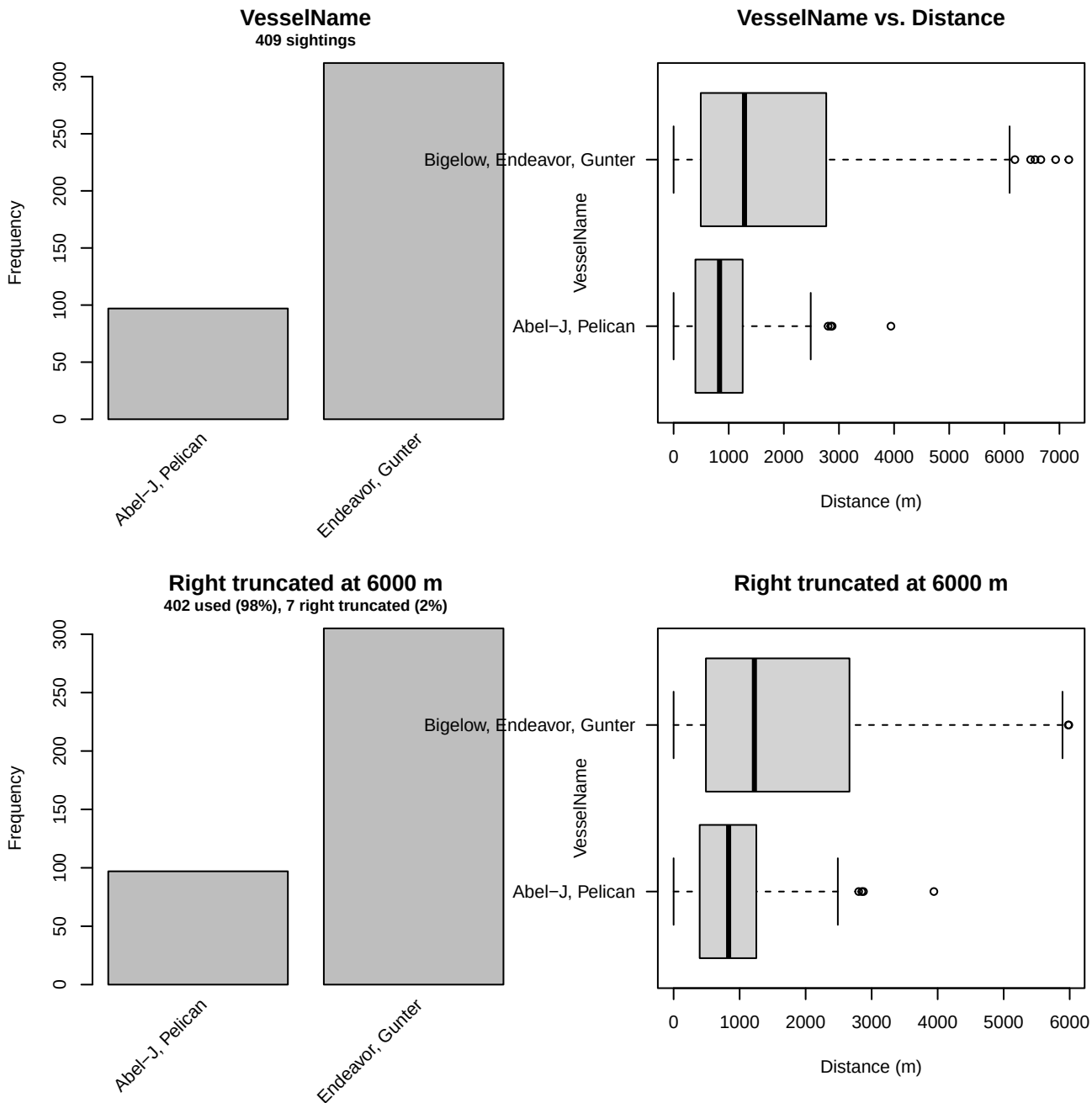

Figure 18: Distribution of the VesselName covariate before (top row) and after (bottom row) observations were truncated to fit the NEFSC detection function.

2.2 Without a Taxonomic Covariate

We fitted the detection functions in this section to pools of species with similar detectability characteristics but could not use a taxonomic identification as a covariate to account for differences between them. We usually took this approach after trying the taxonomic covariate and finding it had insufficient statistical power to be retained. We also resorted to it when the focal taxon being modeled had too few observations to be allocated its own taxonomic covariate level and was too poorly known for us to confidently determine which other taxa we could group it with.

2.2.1 Shipboard Surveys

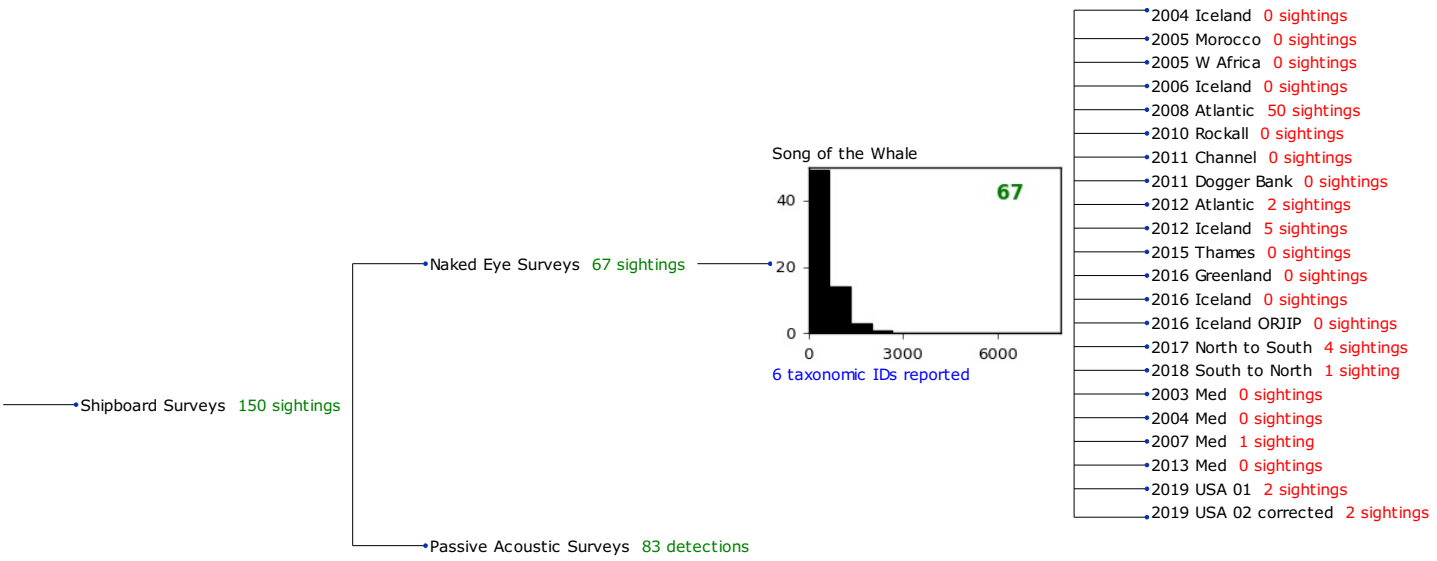

Figure 19: Detection hierarchy for shipboard surveys, showing how they were pooled during detectability modeling, for detection functions that pooled multiple taxa but could not use a taxonomic covariate to account for differences between them. Each histogram represents a detection function and summarizes the perpendicular distances of observations that were pooled to fit it, prior to truncation. Observation counts, also prior to truncation, are shown in green when they met the recommendation of Buckland et al. (2001) that detection functions utilize at least 60 sightings, and red otherwise. For rare taxa, it was not always possible to meet this recommendation, yielding higher statistical uncertainty. During the spatial modeling stage of the analysis, effective strip widths were computed for each survey using the closest detection function above it in the hierarchy (i.e. moving from right to left in the figure). Surveys that do not have a detection function above them in this figure were either addressed by a detection function presented in a different section of this report, or were omitted from the analysis.

2.2.1.1 Song of the Whale

After right-truncating observations greater than 1400 m, we fitted the detection function to the 64 observations that remained (Table 9). The selected detection function (Figure 20) used a hazard rate key function with Beaufort (Figure 21) as a covariate.

Table 9: Observations used to fit the Song of the Whale detection function.

ScientificName	n
Hyperoodon ampullatus	6
Mesoplodon bidens	1
Mesoplodon densirostris	8
Mesoplodon europaeus	1
Ziphiidae	33
Ziphius cavirostris	15
Total	**64**

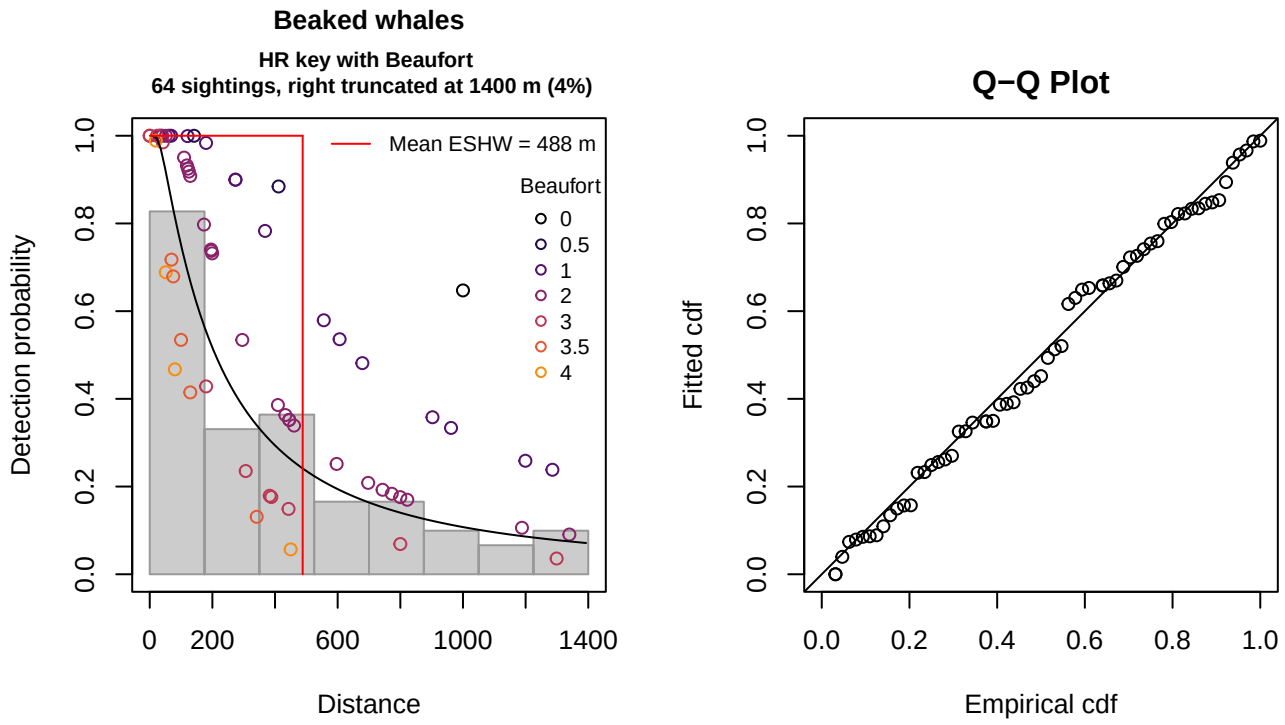

Figure 20: Song of the Whale detection function and Q-Q plot showing its goodness of fit.

Statistical output for this detection function:

```
Summary for ds object
Number of observations :  64
Distance range         :  0  -  1400
AIC                    :  885.1258

Detection function:
 Hazard-rate key function

Detection function parameters
Scale coefficient(s):
             estimate        se
(Intercept)  6.9376582 0.6699448
Beaufort    -0.7220239 0.3032269

Shape coefficient(s):
             estimate        se
(Intercept) 0.3217451 0.2484107

                       Estimate          SE        CV
Average p              0.2647685  0.07532832 0.2845064
N in covered region 241.7206120 74.00931015 0.3061771

Distance sampling Cramer-von Mises test (unweighted)
Test statistic = 0.041284  p = 0.926416
```

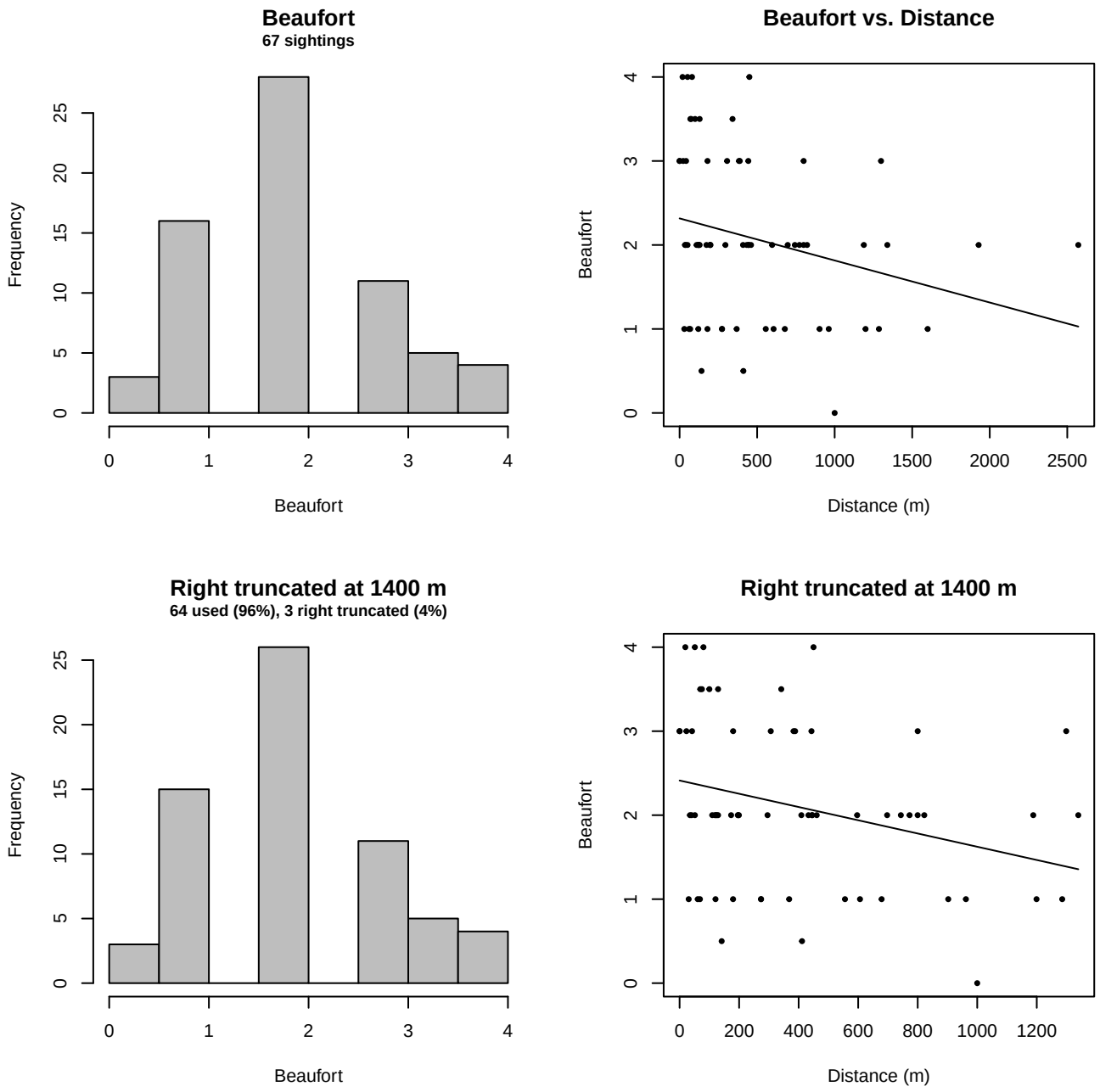

Figure 21: Distribution of the Beaufort covariate before (top row) and after (bottom row) observations were truncated to fit the Song of the Whale detection function.

3 Bias Corrections

Density surface modeling methodology uses *distance sampling* (Buckland et al. 2001) to model the probability that an observer on a line transect survey will detect an animal given the perpendicular distance to it from the transect line. Distance sampling assumes that detection probability is 1 when perpendicular distance is 0. When this assumption is not met, detection probability is biased high, leading to an underestimation of density and abundance. This is known as the $g_0 < 1$ problem, where g_0 refers to the detection probability at distance 0. Modelers often try to address this problem by estimating g_0 empirically and dividing it into estimated density or abundance, thereby correcting those estimates to account for the animals that were presumed missed.

Two important sources of bias for visual surveys are known as *availability bias*, in which an animal was present on the transect line but impossible to detect, e.g. because it was under water, and *perception bias*, in which an animal was present and available but not noticed, e.g. because of its small size or cryptic coloration or behavior (Marsh and Sinclair 1989). Modelers often

estimate the influence of these two sources of bias on detection probability independently, yielding two estimates of g_0, hereafter referred to as g_{0A} and g_{0P}, and multiply them together to obtain a final, combined estimate: $g_0 = g_{0A}.g_{0P}$.

Our overall approach was to perform this correction on a per-observation basis, to have the flexibility to account for many factors such as platform type, surveyor institution, group size, group composition (e.g. singleton, mother-calf pair, or surface active group), and geographic location (e.g. feeding grounds vs. calving grounds). The level of complexity of the corrections varied by species according to the amount of information available, with North Atlantic right whale having the most elaborate corrections, derived from a substantial set of publications documenting its behavior, and various lesser known odontocetes having corrections based only on platform type (aerial or shipboard), derived from comparatively sparse information. Here we document the corrections used for northern bottlenose whale.

3.1 Aerial Surveys

Reflecting the northerly distribution of the species, the only collaborating institution that reported aerial sightings of northern bottlenose whale was NOAA NEFSC (Table 1). Palka et al. (2021) developed a perception bias correction using two team, mark recapture distance sampling (MRDS) methodology (Burt et al. 2014) for beaked whales sighted from aerial surveys conducted in 2010-2017 by NEFSC during the AMAPPS program. We applied this correction to all aerial sightings (all were from NEFSC), including those prior to the AMAPPS program and from the NARWSS program. Palka previously developed a correction for the pre-AMAPPS surveys (Palka 2006) but it utilized older methods and less data than the 2021 analysis, so we used the 2021 analysis instead.

No perception bias estimate was available for NARWSS, but that program used the same aircraft and many of the same observers as the AMAPPS program. However, it flew at a higher altitude and had a searching strategy designed to maximize detections of large whales, so it is possible the AMAPPS estimate undercorrected the NARWSS data (i.e. g_{0P} for NARWSS should have been less than g_{0P} for AMAPPS). If so, it is possible this led to a slight underestimation of density.

We estimated availability bias corrections using the Laake et al. (1997) estimator and dive intervals (Table 11) reported by Hooker et al. (2009) (we averaged all dives (n=179) listed in their Table 2 for Animal Codes Ha_2 and Ha_{28}). To estimate time in view, needed by the Laake estimator, we used results reported by Robertson et al. (2015), rescaled linearly for each survey program according to its target altitude and speed.

To address the influence of group size on availability bias, we applied the group availability estimator of McLellan et al. (2018) on a per-observation basis. Following Palka et al. (2021), who also used that method, we assumed that individuals in the group dived asynchronously. The resulting g_{0A} corrections ranged from about 0.38 to 0.91 (Figure 22). We caution that the assumption of asynchronous diving can lead to an underestimation of density and abundance if diving is actually synchronous; see McLellan et al. (2018) for an exploration of this effect. However, if future research finds that this species conducts synchronous dives and characterizes the degree of synchronicity, the model can be updated to account for this knowledge.

Table 10: Perception bias corrections for northern bottlenose whale applied to aerial surveys.

Surveys	Group Size	g_{0P}	g_{0P} Source
NEFSC	Any	0.62	Palka et al. (2021): NEFSC

Table 11: Surface and dive intervals for northern bottlenose whale used to estimate availability bias corrections.

Surface Interval (s)	Dive Interval (s)	Source
90.1	444	Hooker et al. (2009)

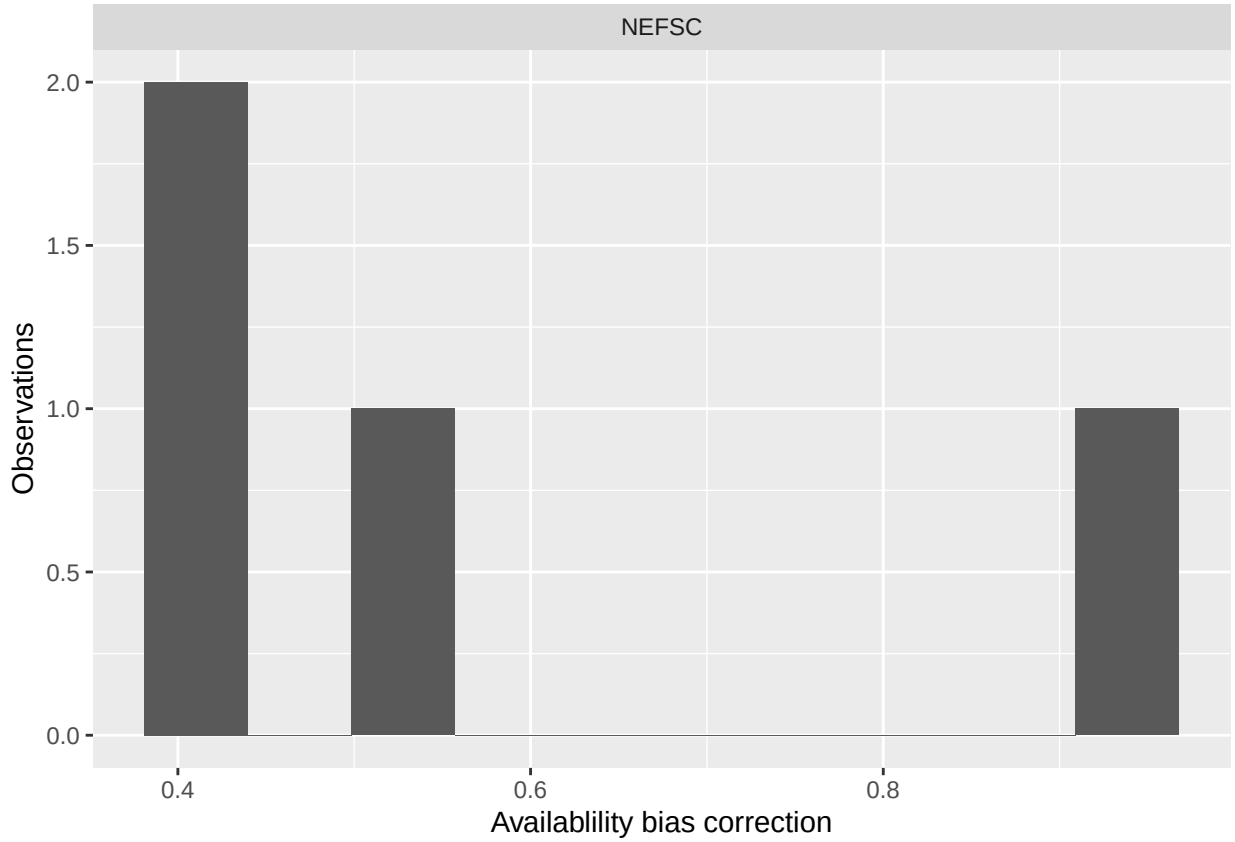

Figure 22: Availability bias corrections for northern bottlenose whale for aerial surveys, by institution.

3.2 Shipboard Surveys

Most of the shipboard surveys in our analysis used high-power (25x150), pedestal-mounted binoculars. Similar to aerial surveys, the only institution that reported sightings of Atlantic white-sided dolphins during high-power binocular surveys was NOAA NEFSC. Palka et al. (2021) developed perception bias corrections using two team, MRDS methodology (Burt et al. 2014) for beaked whales sighted from high-power binocular surveys conducted in 2010-2017 by NEFSC during the AMAPPS program. We applied this correction to all high-power binocular sightings (all were from NEFSC), including those prior to the AMAPPS program. Palka previously developed a correction for the pre-AMAPPS surveys (Palka 2006) but that was specific to northern bottlenose whale but it utilized older methods than the 2021 analysis and only 3 sightings, so we used the 2021 analysis instead.

For the MCR Song of the Whale surveys, which searched by naked eye, we applied the perception bias estimate developed by Leonard and Øien (2020) for shipboard surveys in the eastern North Atlantic. This was the only perception bias estimate we could locate for northern bottlenose whales observed by naked eye, and we caution that the observation height for the Song of the Whale (5.3 m) was substantially lower than for the two platforms in Leonard's analysis (11.8 m and 9.7 m).

Although the northern bottlenose whale is reported to undertake very deep and long dives (Hooker et al. 1999), the mean dive interval of 7.4 min that we derived from the results of Hooker et al. (2009) is relatively short compared to other beaked whales, such as Cuvier's beaked whale, for which Palka et al. (2021) reported a mean dive interval of 34.44 min. The northern bottlenose whale's interval was actually less than that of short-finned pilot whale (daytime, 9.00 min) in Palka's analysis. Given that, and that Palka estimated a shipboard availability bias correction of $g_{0A} = 1$ for short-finned pilot whales, we assumed the same for northern bottlenose whales.

Table 12: Perception and availability bias corrections for northern bottlenose whale applied to shipboard surveys.

Surveys	Searching Method	Group Size	g_{0P}	g_{0P} Source	g_{0A}	g_{0A} Source
NEFSC	Binoculars	Any	0.42	Palka et al. (2021): NEFSC	1	Assumed
MCR	Naked Eye	Any	0.85	Leonard and Oien (2020)	1	Assumed

4 Geographic Strata

With so few sightings, it was not possible to fit a traditional density surface model that related density observed on survey segments to environmental covariates. Nor was it possible to make proper design-based abundance estimates using traditional distance sampling (Buckland et al. 2001), because the aggregate surveys provided very heterogeneous coverage that did not together constitute a proper systematic survey design.

To provide interested parties with at least rough estimates of density in ecologically relevant geographic strata, we first split the study area into five strata (Figure 1) at major habitat boundaries. We placed our first split at the continental shelf break, defined as the 100 meter isobath, separating the study area in into shelf and offshore regions. (We manually cut across the Northeast Channel of the Gulf of Maine, so that the Gulf was considered part of the shelf.) We then split the shelf region at Cape Hatteras, a location where the Gulf Stream separates from the continental shelf, which has previously been used to delineate community structure in marine mammals (Schick et al. 2011). We also split the shelf region at the Nantucket Shoals, which separate the Gulf of Maine from the New York Bight. We split off the bays and sounds of New York, Rhode Island, and southern Massachusetts, generally at the 10 m isobath, on the basis that these inshore areas are rarely visited by cetaceans of any species. Finally, we split the offshore region at the north wall of the Gulf Stream, starting at Cape Hatteras and extending along the north wall of the Gulf Stream, as defined with a long-term climatology of total kinetic energy, to the edge of the study area.

We then derived density estimates for each stratum by fitting a model with no covariates, under the assumption that density would be distributed uniformly within the stratum. This assumption, if true, would mean we would obtain similar density estimates for a given stratum under any sampling design, and therefore it would not matter if there was some heterogeneity in sampling within the stratum. However, we strongly caution that this assumption did not hold for the other, more-common species we successfully modeled with traditional density surface modeling, as evidenced by the non-uniform patterns in density predicted by those species' models. That said, when those results are viewed at a very coarse, ecoregional scale, the boundaries used here often correlate with boundaries or strong gradients in density in those models. Thus, for the much rarer species, such as northern bottlenose whale documented here, we offer this simplified approach as a rough-and-ready substitute for a full density surface model.

In this section, we present maps of each stratum that contained sightings, with tallies of effort and sightings that occurred.

4.1 Offshore North of Gulf Stream

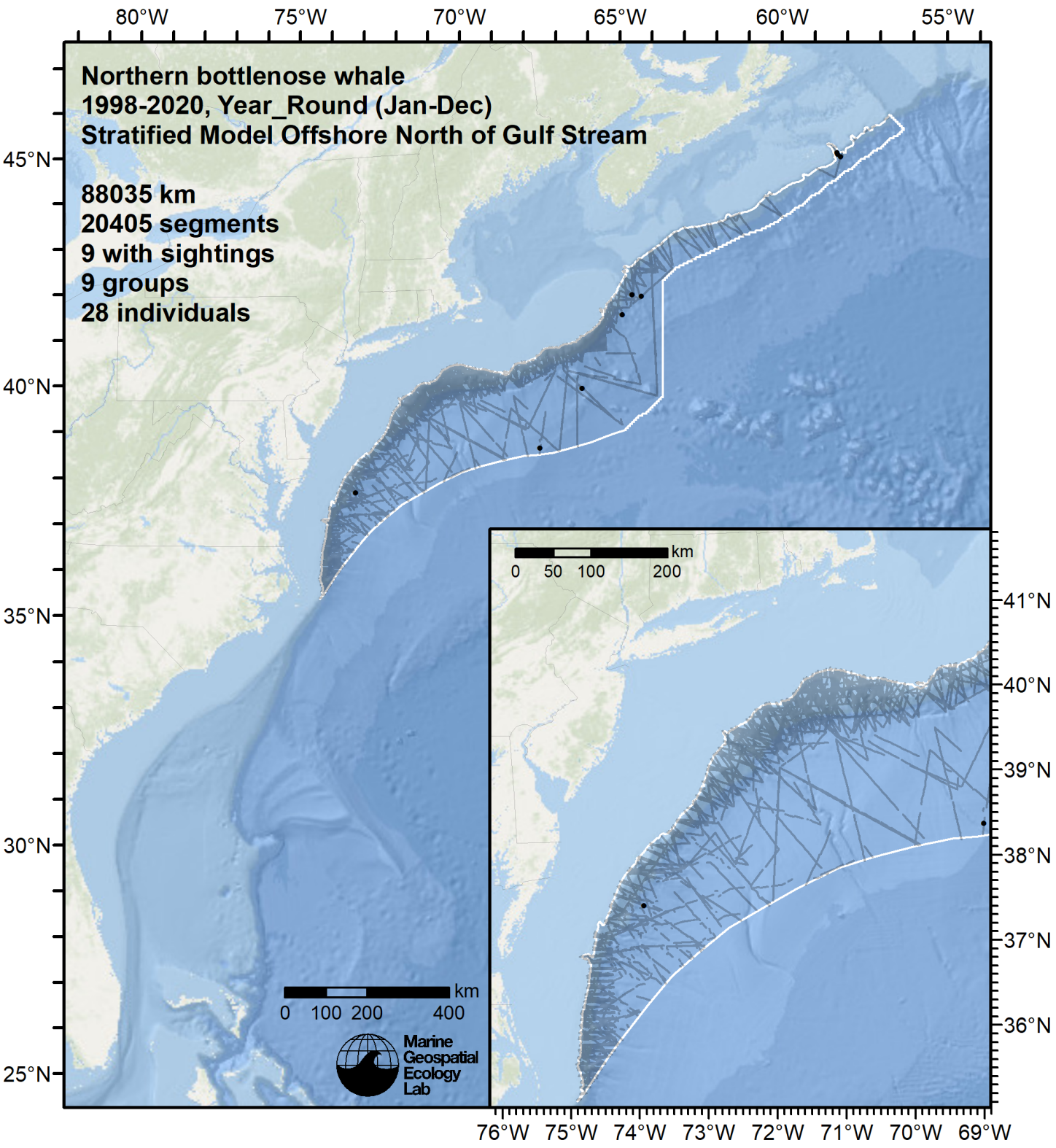

Figure 23: Survey segments and sightings used to estimate northern bottlenose whale density for the "Offshore North of Gulf Stream" region. Black points indicate segments with observations.

5 Predictions

5.1 Summarized Predictions

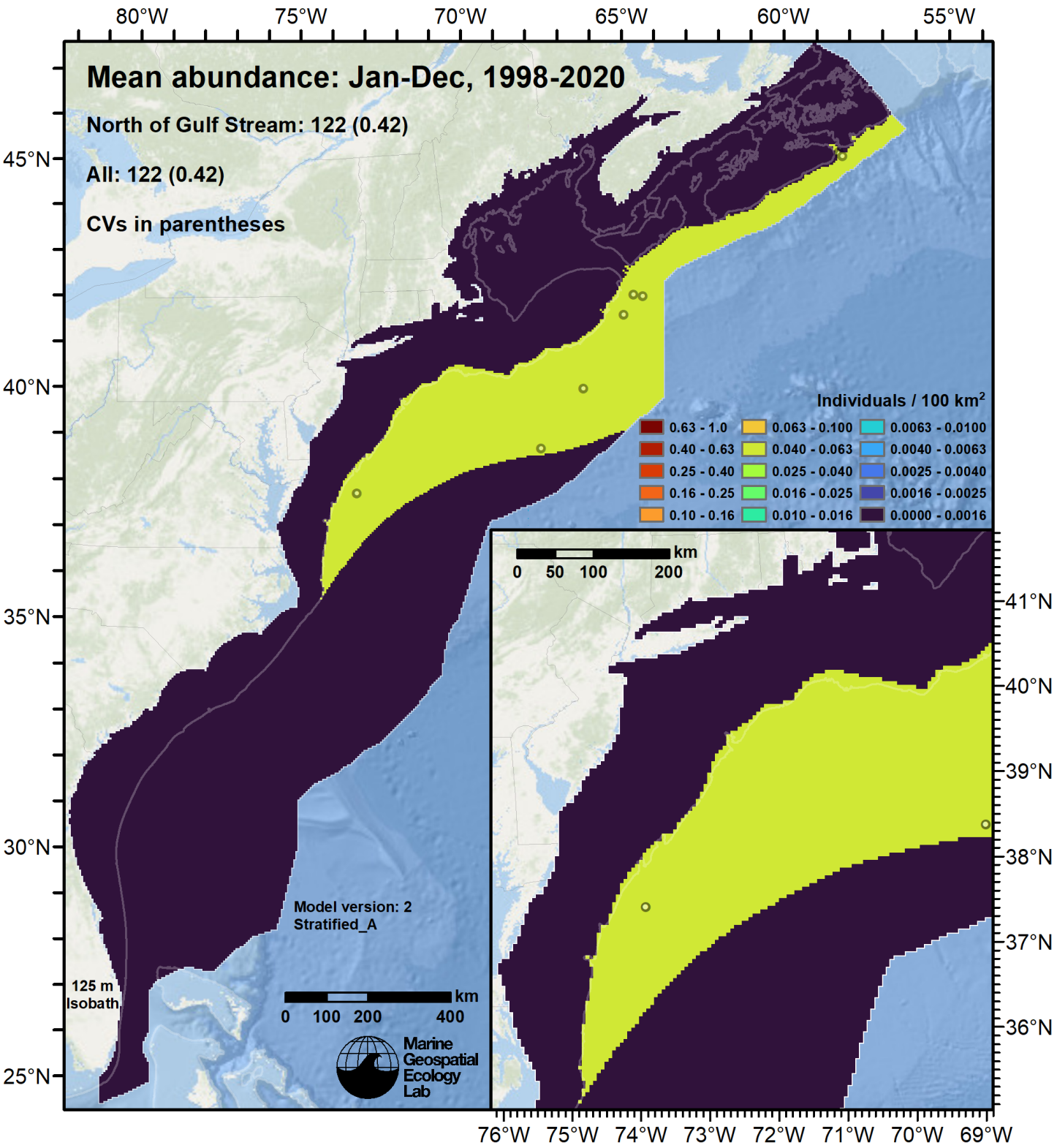

Figure 24: Northern bottlenose whale density estimated for the indicated period. Open circles indicate segments with observations. The abundance estimate and its coefficient of variation (CV) are given in the subtitle.

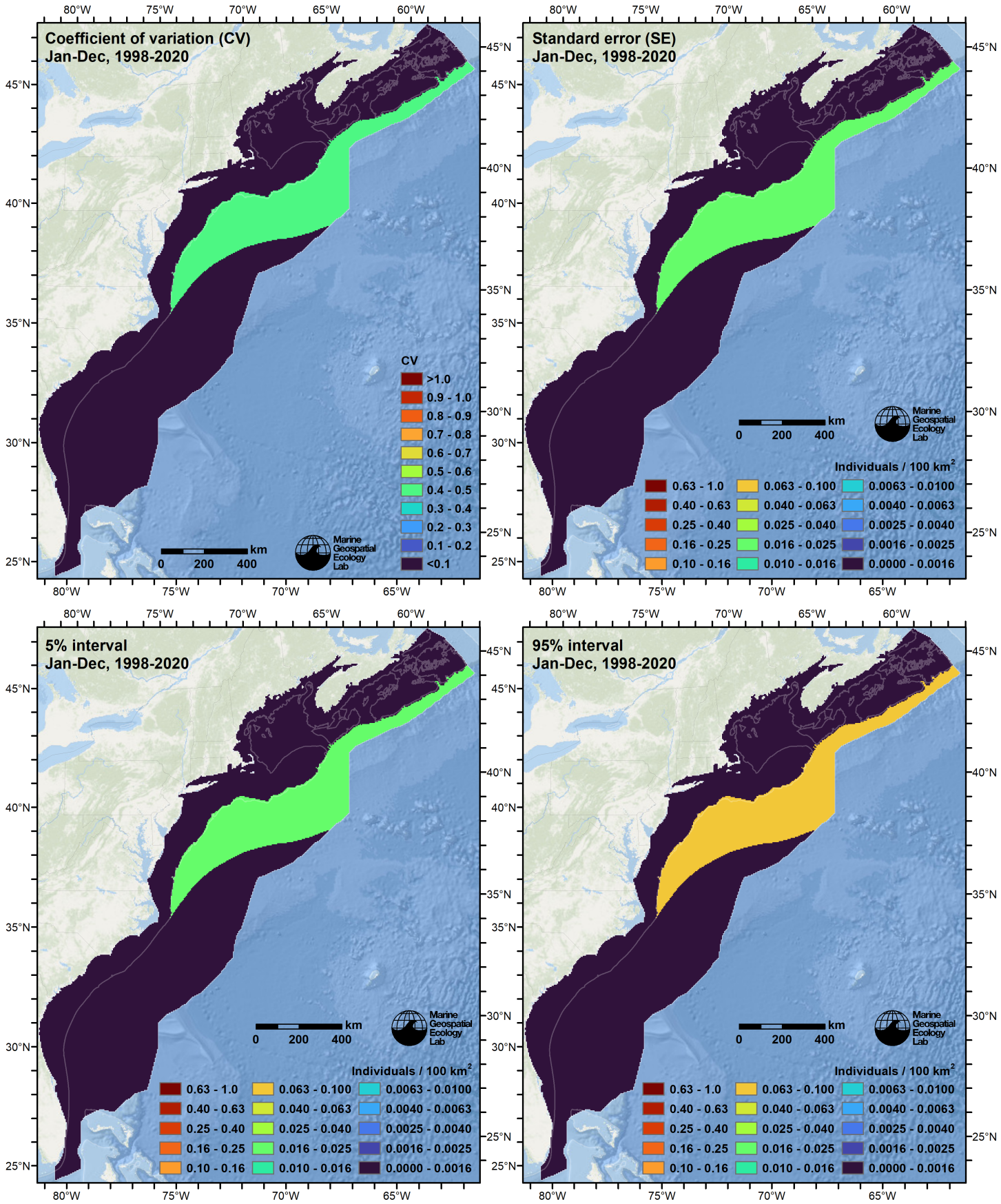

Figure 25: Uncertainty statistics for the northern bottlenose whale estimated density surface (Figure 24).

Table 13: Northern bottlenose whale abundance and density estimated for each stratum.

Region	Abundance	CV	95% Interval	Area (km^2)	Density (indiv. / 100 km^2)
Offshore Gulf Stream and South	0	0.000	0 - 0	499,300	0.0000
Offshore North of Gulf Stream	122	0.417	56 - 267	253,575	0.0480
Shelf Cape Hatt. to Nant. Shoals	0	0.000	0 - 0	104,425	0.0000
Shelf North of Nantucket Shoals	0	0.000	0 - 0	302,025	0.0000
Shelf South of Cape Hatteras	0	0.000	0 - 0	105,500	0.0000
Sounds of NY, RI, and MA	0	0.000	0 - 0	8,600	0.0000
Total	122	0.417	56 - 267	1,273,425	0.0096

5.2 Abundance Comparisons

5.2.1 NOAA Stock Assessment Report

At the time of this writing, the 2014 Stock Assessment Report (SAR) was the most recent to examine the northern bottlenose whale (Waring et al. 2015). It reported that "The total number of northern bottlenose whales off the eastern U.S. coast is unknown." Thus, no SAR estimate is available for comparison.

5.2.2 Previous Density Model

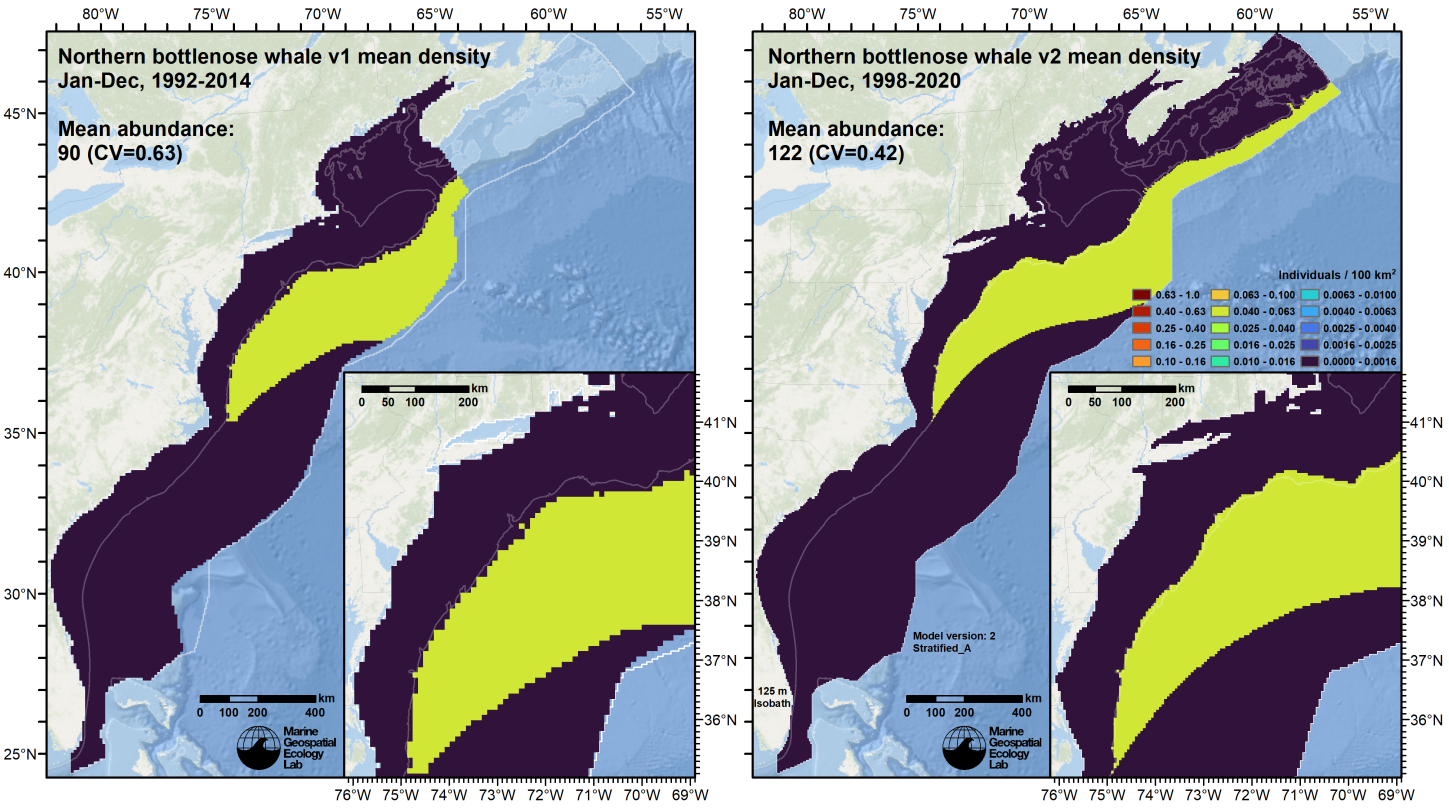

Figure 26: Comparison of the mean density predictions from the previous model (left) released by Roberts et al. (2016) to those from this model (right).

6 Discussion

A 2012 review of northern bottlenose whale population structure in the North Atlantic reported that they are found north of approximately 37.5 °N and deeper than 500 m, but seem to prefer depths between 800-1800 m along the continental slope (Whitehead and Hooker 2012). They are extremely uncommon or rare in waters of the U.S. Exclusive Economic Zone (Waring

et al. 2015). Farther north, along the Scotian Shelf, they are more common, especially near submarine canyons known as the Gully, Shortland Canyon, and Haldimand Canyon (Wimmer and Whitehead 2004). Periodic acoustic monitoring of the shelf break at various locations between Florida and the Gully during 2015-2020 with methods designed to detect northern bottlenose whales only detected them at the Gully (Stanistreet et al. 2017; Weiss et al. 2021; Kowarski et al. 2022), although some of the recorders in southern half of this region were deployed at depths shallower than 500 m. The Scotian Shelf population appears to be genetically distinct from the two other closest known populations, in northern Labrador and northern Iceland (Dalebout et al. 2006). Northern bottlenose whales are not believed to migrate, at least in the western North Atlantic (Whitehead and Hooker 2012), and exhibit relatively small daily movements compared to other large pelagic species (Wimmer and Whitehead 2004).

Three of the sightings incorporated into our analysis were in the Gully. The remaining seven occurred between northeastern Georges Bank and Maryland, at with the southernmost occurring at 37.67 °N. All sightings were in waters over 1000 m deep near high-relief bathymetric features including canyons and seamounts. This overall distribution agrees with the habitat described above. However, one sighting was made over 180 km from shelf break, at 38.399 °N, 68.625 °W, near the north wall of the Gulf Stream, within 8 km of Veatch Canyon in water over 3900 m deep. This suggests the species can occur quite far from the intermediate-depth, high-relief areas along the shelf edge, and supports our use of the Gulf Stream as a defining feature for the species' habitat.

The NOAA Stock Assessment Reports have never listed an abundance estimate for the U.S. east coast. However, the mean size of the Scotian Shelf population was estimated by photo identification mark-recapture methodology by Whitehead and Wimmer (2005) at 163 whales, and again with updated data and methods by O'Brien and Whitehead (2013) at 143 whales. Our prior estimate, 90 whales, for offshore waters north of the Gulf Stream did not include any sightings along the Scotian Shelf and we excluded it from the spatial extent of the estimate (Roberts et al. 2016). Our new estimate, 122 whales, included three sightings on the Scotian Shelf so we included the Scotian Shelf in our new spatial extent. Density increased, from 0.0406 individuals 100 km^{-2} to 0.0480 individuals 100 km^{-2} (Figure 26). We investigated the possibility of further splitting the modeled region into two, so that the Scotian Shelf would have its own estimate, but we judged effort too low along the Scotian Shelf to allow this. Given that our estimate for both U.S. waters and the Scotian Shelf together is lower than the mark-recapture estimates just for the Scotian Shelf, we strongly caution that our model likely underestimates density along the Scotian Shelf, and recommend that assessments of potential impacts from human activities to northern bottlenose whales there consider the mark-recapture estimates. Our stratified modeling approach does not fully correct for the heterogeneous distribution of sampling effort in space in time, which could have biased our abundance estimate (see Section 4).

References

Barco SG, Burt L, DePerte A, Digiovanni R Jr. (2015) Marine Mammal and Sea Turtle Sightings in the Vicinity of the Maryland Wind Energy Area July 2013-June 2015, VAQF Scientific Report #2015-06. Virginia Aquarium & Marine Science Center Foundation, Virginia Beach, VA

Buckland ST, Anderson DR, Burnham KP, Laake JL, Borchers DL, Thomas L (2001) Introduction to Distance Sampling: Estimating Abundance of Biological Populations. Oxford University Press, Oxford, UK

Burt ML, Borchers DL, Jenkins KJ, Marques TA (2014) Using mark-recapture distance sampling methods on line transect surveys. Methods in Ecology and Evolution 5:1180–1191. doi: 10.1111/2041-210X.12294

Cole T, Gerrior P, Merrick RL (2007) Methodologies of the NOAA National Marine Fisheries Service Aerial Survey Program for Right Whales (Eubalaena glacialis) in the Northeast U.S., 1998-2006. U.S. Department of Commerce, Woods Hole, MA

Cotter MP (2019) Aerial Surveys for Protected Marine Species in the Norfolk Canyon Region: 2018–2019 Final Report. HDR, Inc., Virginia Beach, VA

Dalebout ML, Ruzzante DE, Whitehead H, ØIen NI (2006) Nuclear and mitochondrial markers reveal distinctiveness of a small population of bottlenose whales (Hyperoodon ampullatus) in the western North Atlantic. Molecular ecology 15:3115–3129.

Foley HJ, Paxton CGM, McAlarney RJ, Pabst DA, Read AJ (2019) Occurrence, Distribution, and Density of Protected Species in the Jacksonville, Florida, Atlantic Fleet Training and Testing (AFTT) Study Area. Duke University Marine Lab, Beaufort, NC

Garrison LP, Martinez A, Maze-Foley K (2010) Habitat and abundance of cetaceans in Atlantic Ocean continental slope waters off the eastern USA. Journal of Cetacean Research and Management 11:267–277.

Hooker SK, Whitehead H, Gowans S (1999) Marine Protected Area Design and the Spatial and Temporal Distribution of Cetaceans in a Submarine Canyon. Conservation Biology 13:592–602. doi: 10.1046/j.1523-1739.1999.98099.x

Hooker SK, Baird RW, Fahlman A (2009) Could beaked whales get the bends? Respiratory Physiology & Neurobiology 167:235–246. doi: 10.1016/j.resp.2009.04.023

Kowarski KA, Martin SB, Maxner EE, Lawrence CB, Delarue JJ-Y, Miksis-Olds JL (2022) Cetacean acoustic occurrence on the US Atlantic Outer Continental Shelf from 2017 to 2020. Marine Mammal Science mms.12962. doi: 10.1111/mms.12962

Laake JL, Calambokidis J, Osmek SD, Rugh DJ (1997) Probability of Detecting Harbor Porpoise From Aerial Surveys: Estimating g(0). Journal of Wildlife Management 61:63–75. doi: 10.2307/3802415

Leiter S, Stone K, Thompson J, Accardo C, Wikgren B, Zani M, Cole T, Kenney R, Mayo C, Kraus S (2017) North Atlantic right whale Eubalaena glacialis occurrence in offshore wind energy areas near Massachusetts and Rhode Island, USA. Endang Species Res 34:45–59. doi: 10.3354/esr00827

Leonard D, Øien N (2020) Estimated Abundances of Cetacean Species in the Northeast Atlantic from Norwegian Shipboard Surveys Conducted in 2014–2018. NAMMCOSP. doi: 10.7557/3.4694

Mallette SD, Lockhart GG, McAlarney RJ, Cummings EW, McLellan WA, Pabst DA, Barco SG (2014) Documenting Whale Migration off Virginia's Coast for Use in Marine Spatial Planning: Aerial and Vessel Surveys in the Proximity of the Virginia Wind Energy Area (VA WEA), VAQF Scientific Report 2014-08. Virginia Aquarium & Marine Science Center Foundation, Virginia Beach, VA

Mallette SD, Lockhart GG, McAlarney RJ, Cummings EW, McLellan WA, Pabst DA, Barco SG (2015) Documenting Whale Migration off Virginia's Coast for Use in Marine Spatial Planning: Aerial Surveys in the Proximity of the Virginia Wind Energy Area (VA WEA) Survey/Reporting Period: May 2014 - December 2014, VAQF Scientific Report 2015-02. Virginia Aquarium & Marine Science Center Foundation, Virginia Beach, VA

Mallette SD, McAlarney RJ, Lockhart GG, Cummings EW, Pabst DA, McLellan WA, Barco SG (2017) Aerial Survey Baseline Monitoring in the Continental Shelf Region of the VACAPES OPAREA: 2016 Annual Progress Report. Virginia Aquarium & Marine Science Center Foundation, Virginia Beach, VA

Marsh H, Sinclair DF (1989) Correcting for Visibility Bias in Strip Transect Aerial Surveys of Aquatic Fauna. The Journal of Wildlife Management 53:1017. doi: 10.2307/3809604

McAlarney R, Cummings E, McLellan W, Pabst A (2018) Aerial Surveys for Protected Marine Species in the Norfolk Canyon Region: 2017 Annual Progress Report. University of North Carolina Wilmington, Wilmington, NC

McLellan WA, McAlarney RJ, Cummings EW, Read AJ, Paxton CGM, Bell JT, Pabst DA (2018) Distribution and abundance of beaked whales (Family Ziphiidae) Off Cape Hatteras, North Carolina, U.S.A. Marine Mammal Science. doi: 10.1111/mms.12500

Mullin KD, Fulling GL (2003) Abundance of cetaceans in the southern U.S. North Atlantic Ocean during summer 1998. Fishery Bulletin 101:603–613.

O'Brien K, Whitehead H (2013) Population analysis of Endangered northern bottlenose whales on the Scotian Shelf seven years after the establishment of a Marine Protected Area. Endang Species Res 21:273–284. doi: 10.3354/esr00533

O'Brien O, Pendleton DE, Ganley LC, McKenna KR, Kenney RD, Quintana-Rizzo E, Mayo CA, Kraus SD, Redfern JV (2022) Repatriation of a historical North Atlantic right whale habitat during an era of rapid climate change. Sci Rep 12:12407. doi: 10.1038/s41598-022-16200-8

Palka D, Aichinger Dias L, Broughton E, Chavez-Rosales S, Cholewiak D, Davis G, DeAngelis A, Garrison L, Haas H, Hatch J, Hyde K, Jech M, Josephson E, Mueller-Brennan L, Orphanides C, Pegg N, Sasso C, Sigourney D, Soldevilla M, Walsh H (2021) Atlantic Marine Assessment Program for Protected Species: FY15 – FY19 (OCS Study BOEM 2021-051). U.S. Deptartment of the Interior, Bureau of Ocean Energy Management, Washington, DC

Palka DL (2006) Summer abundance estimates of cetaceans in US North Atlantic navy operating areas (NEFSC Reference Document 06-03). U.S. Department of Commerce, Northeast Fisheries Science Center, Woods Hole, MA

Palka DL, Chavez-Rosales S, Josephson E, Cholewiak D, Haas HL, Garrison L, Jones M, Sigourney D, Waring G, Jech M, Broughton E, Soldevilla M, Davis G, DeAngelis A, Sasso CR, Winton MV, Smolowitz RJ, Fay G, LaBrecque E, Leiness JB, Dettloff K, Warden M, Murray K, Orphanides C (2017) Atlantic Marine Assessment Program for Protected Species: 2010-2014 (OCS Study BOEM 2017-071). U.S. Deptartment of the Interior, Bureau of Ocean Energy Management, Washington, DC

Quintana-Rizzo E, Leiter S, Cole T, Hagbloom M, Knowlton A, Nagelkirk P, O'Brien O, Khan C, Henry A, Duley P, Crowe L, Mayo C, Kraus S (2021) Residency, demographics, and movement patterns of North Atlantic right whales Eubalaena

glacialis in an offshore wind energy development area in southern New England, USA. Endang Species Res 45:251–268. doi: 10.3354/esr01137

Read AJ, Barco S, Bell J, Borchers DL, Burt ML, Cummings EW, Dunn J, Fougeres EM, Hazen L, Hodge LEW, Laura A-M, McAlarney RJ, Peter N, Pabst DA, Paxton CGM, Schneider SZ, Urian KW, Waples DM, McLellan WA (2014) Occurrence, distribution and abundance of cetaceans in Onslow Bay, North Carolina, USA. Journal of Cetacean Research and Management 14:23–35.

Redfern JV, Kryc KA, Weiss L, Hodge BC, O'Brien O, Kraus SD, Quintana-Rizzo E, Auster PJ (2021) Opening a Marine Monument to Commercial Fishing Compromises Species Protections. Front Mar Sci 8:645314. doi: 10.3389/fmars.2021.645314

Roberts JJ, Best BD, Mannocci L, Fujioka E, Halpin PN, Palka DL, Garrison LP, Mullin KD, Cole TVN, Khan CB, McLellan WA, Pabst DA, Lockhart GG (2016) Habitat-based cetacean density models for the U.S. Atlantic and Gulf of Mexico. Scientific Reports 6:22615. doi: 10.1038/srep22615

Roberts JJ, Yack TM, Halpin PN (2023) Marine mammal density models for the U.S. Navy Atlantic Fleet Training and Testing (AFTT) study area for the Phase IV Navy Marine Species Density Database (NMSDD), Document Version 1.3. Duke University Marine Geospatial Ecology Lab, Durham, NC

Robertson FC, Koski WR, Brandon JR, Thomas TA, Trites AW (2015) Correction factors account for the availability of bowhead whales exposed to seismic operations in the Beaufort Sea. Journal of Cetacean Research and Management 15:35–44.

Ryan C, Boisseau O, Cucknell A, Romagosa M, Moscrop A, McLanaghan R (2013) Final report for trans-Atlantic research passages between the UK and USA via the Azores and Iceland, conducted from R/V Song of the Whale 26 March to 28 September 2012. Marine Conservation Research International, Essex, UK

Schick R, Halpin P, Read A, Urban D, Best B, Good C, Roberts J, LaBrecque E, Dunn C, Garrison L, Hyrenbach K, McLellan W, Pabst D, Palka D, Stevick P (2011) Community structure in pelagic marine mammals at large spatial scales. Marine Ecology Progress Series 434:165–181. doi: 10.3354/meps09183

Stanistreet JE, Nowacek DP, Baumann-Pickering S, Bell JT, Cholewiak DM, Hildebrand JA, Hodge LEW, Moors-Murphy HB, Van Parijs SM, Read AJ (2017) Using passive acoustic monitoring to document the distribution of beaked whale species in the western North Atlantic Ocean. Canadian Journal of Fisheries and Aquatic Sciences 1–12. doi: 10.1139/cjfas-2016-0503

Stone KM, Leiter SM, Kenney RD, Wikgren BC, Thompson JL, Taylor JKD, Kraus SD (2017) Distribution and abundance of cetaceans in a wind energy development area offshore of Massachusetts and Rhode Island. J Coast Conserv 21:527–543. doi: 10.1007/s11852-017-0526-4

Torres LG, Mclellan WA, Meagher E, Pabst DA (2005) Seasonal distribution and relative abundance of bottlenose dolphins, Tursiops truncatus, along the US mid-Atlantic coast. Journal of Cetacean Research and Management 7:153.

Waring GT, Josephson E, Maze-Foley K, Rosel PE, Byrd B, Cole TVN, Engleby L, Garrison LP, Hatch J, Henry A, Horstman SC, Litz J, Mullin KD, Orphanides C, Pace RM, Palka DL, Lyssikatos MC, Wenzel FW (2015) US Atlantic and Gulf of Mexico Marine Mammal Stock Assessments - 2014. NOAA National Marine Fisheries Service, Northeast Fisheries Science Center, Woods Hole, MA

Weiss SG, Cholewiak D, Frasier KE, Trickey JS, Baumann-Pickering S, Hildebrand JA, Van Parijs SM (2021) Monitoring the acoustic ecology of the shelf break of Georges Bank, Northwestern Atlantic Ocean: New approaches to visualizing complex acoustic data. Marine Policy 130:104570. doi: 10.1016/j.marpol.2021.104570

Whitehead H, Hooker S (2012) Uncertain status of the northern bottlenose whale Hyperoodon ampullatus: Population fragmentation, legacy of whaling and current threats. Endangered Species Research 19:47–61. doi: 10.3354/esr00458

Whitehead H, Wimmer T (2005) Heterogeneity and the mark recapture assessment of the Scotian Shelf population of northern bottlenose whales (Hyperoodon ampullatus). Canadian Journal of Fisheries and Aquatic Sciences 62:2573–2585.

Wimmer T, Whitehead H (2004) Movements and distribution of northern bottlenose whales, Hyperoodon ampullatus, on the Scotian Slope and in adjacent waters. Canadian Journal of Zoology 82:1782–1794.

Zoidis AM, Lomac-MacNair KS, Ireland DS, Rickard ME, McKown KA, Schlesinger MD (2021) Distribution and density of six large whale species in the New York Bight from monthly aerial surveys 2017 to 2020. Continental Shelf Research 230:104572. doi: 10.1016/j.csr.2021.104572